HHS Public Access

Author manuscript

ACS Nano. Author manuscript; available in PMC 2021 October 27.

Published in final edited form as:

ACS Nano. 2020 October 27; 14(10): 12291–12312. doi:10.1021/acsnano.0c06017.

Moving Electrons Purposefully through Single Molecules and Nanostructures: A Tribute to the Science of Nongjian Tao

Erica S. Forzani[1], **Huixin He**[2], **Josh Hihath**[3], **Stuart Lindsay**[4], **Reginald M. Penner**[5], **Shaopeng Wang**[6], **Bingqian Xu**[7]

[1]Biodesign Center for Bioelectronics and Biosensors, Departments of Chemical Engineering and Mechanical Engineering, Arizona State University, Tempe, Arizona 85287, United States

[2]Department of Chemistry, Rutgers University, Newark, New Jersey 07102, United States

[3]Department of Electrical and Computer Engineering, University of California, Davis, Davis, CA 95616, United States

[4]Biodesign Center for Single Molecule Biophysics, Arizona State University, Tempe, Arizona 85287, United States

[5]Department of Chemistry, University of California, Irvine, California 92697, United States

[6]Biodesign Center for Bioelectronics and Biosensors, Arizona State University, Tempe, Arizona 85287, United States

[7]School of Electrical and Computer Engineering, University of Georgia, Athens, Georgia 30602, United States

Abstract

Electrochemistry intersected nanoscience 25 years ago when it became possible to control the flow of electrons through single molecules and nanostructures. Many surprises and a wealth of understanding were generated by these experiments. Nongjian Tao was among the pioneering scientists who created the methods and technologies for advancing this new frontier. Achieving deeper understanding of charge transport in molecules and low-dimensional materials was the first priority of his experiments, but he also succeeded in discovering applications in chemical sensing and biosensing for these novel nanoscopic systems. In parallel with this work, the investigation of a range of phenomena using novel optical microscopic methods was a passion of Nongjian and his students. This article is a review and an appreciation of some of his many contributions with a view to the future.

Graphical Abstract

rmpenner@uci.edu.

DEDICATION

This article is dedicated to the memory of our beloved friend and mentor Prof. Nongjian Tao (15 September 1963–15 March 2020).

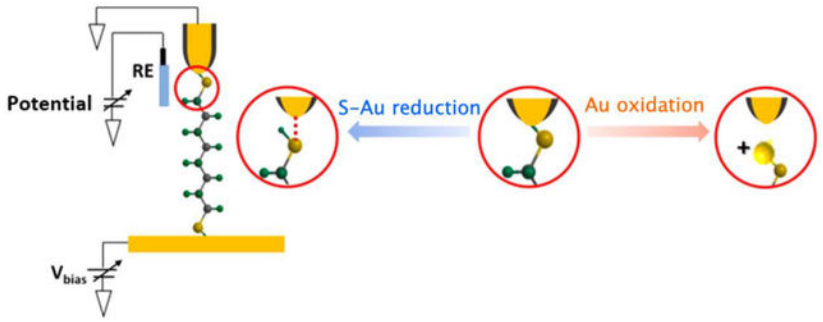

Keywords

STM; AFM; nanoscience; electrochemistry; microscopy; surface plasmon resonance

Professor Nongjian Tao (“NJ”, Figure 1) of Arizona State University (ASU) passed away on March 15, 2020 at the age of 56.[1] He was an extraordinary scholar and scientist whose insightful and influential work encompassed a wide range of nanoscale phenomena in electrochemistry, surface science, chemical and biological analysis, electrical engineering, and quantum physics. In this scientific remembrance we recount some of his beautiful and impactful science.

This article is organized chronologically, representing the major areas in which his research group worked. His contributions in these areas overlapped in time, as he developed new research thrusts in his group, especially as his group expanded and diversified at ASU, so this chronology is approximate. In fact, NJ progressively *added* new research areas without abandoning many over his career. At Florida International University and ASU in the early 1990s, he pioneered scanning tunneling microscopy (STM) and atomic force microscopy (AFM) investigations of molecular monolayers in electrochemical environments.[2–9] This work led to a brief period, in the late 1990s and early 2000s, during which he investigated transport through single metal[10–12] and polymer[13–19] nanowires prepared between a surface and an STM or AFM tip in electrochemical environments.

Those experiments spawned two research directions that would define his career. The first was the development of an array of analytical methods that followed from advances in surface plasmon resonance (SPR) spectroscopy (1999–2010 and beyond)[20,21,30–32,22–29] and the re-purposing of polymer nanojunctions for chemical analyses (in 2003).[14,33–35] The second research direction was transport studies of single molecules using the STM-break junction (STM-BJ) methodology invented in his group (initiated in the 2003 time frame).[36–42]

The STM-BJ methodology for investigating transport through single molecules was applied to DNA almost immediately after its discovery, in 2004.[41,43–49] This period coincided with the publication of a number of studies from other research groups in which charge transport through DNA was probed.[50–57] Subsequently, this subfield would become a productive one for his research group.

Following contributions to SPR techniques earlier in his career, optical microscopy methods, often hyphenated with other methods, emerged as an emphasis of his program in recent years.[31,58–66] One success involved the application of “differential detection”, used to enhance the sensitivity of force measurement in an AFM system, to surface plasmon spectroscopy.[24,67–71] This invention led to his successful development of new and powerful functional imaging tools. NJ also devoted time and effort to the translation of his research to broad societal benefit, co-founding two companies with his former students and postdocs.

SCANNING TUNNELING MICROSCOPY AND ATOMIC FORCE MICROSCOPY OF MOLECULES IN ELECTROCHEMICAL ENVIRONMENTS

As a graduate student at ASU, NJ studied low-frequency modes in DNA and other condensed matter systems, completing his PhD in 1988.[72–77] He went on to initiate studies of disordered systems as a postdoc in the lab of the late Professor Herman Cummins at CUNY. Heeding the pleas of his thesis advisor, he returned to ASU in 1990. The ASU lab had started a new research program, utilizing STM to image surfaces and molecules under aqueous solutions.[3] It was here that NJ began his successful merger of electrochemistry and nanoscience, exploiting the development of large, flat single crystal gold surfaces that were readily cleaned with a hydrogen flame to yield near-perfect single-crystal voltammety.[78] NJ used these surfaces in electrochemical STM to study surface reconstruction,[79] potential-induced phase transitions[80], controlled deposition of lead[81] and halides,[82] and, returning to the theme of his PhD, an exquisite study of the phases of DNA bases adsorbed on Au(111) under potential control.[83] He also helped to perfect AFM as an electrochemical tool.[84,85] As a graduate student, NJ had used Brillioun scattering to map the microelastic properties of bone, a material whose properties are dominated by micro- and nanoscale heterogeneity.[86] He returned to this problem with one of the first AFM studies to map these elastic heterogeneities on the nanoscale.[72]

In 1992, NJ started his independent career at Florida International University (FIU). At that point, STM and AFM had been in use for several years as imaging tools to study surface morphology at the molecular and atomic scales, but efforts to understand the imaging of redox-active molecules in solution were still at an early stage, impeded by practical experimental problems. Operating an STM in an electrochemical environment with separate control of the surface potential *versus* a reference electrode presented practical problems because applied voltages in the STM could drive the reactions of redox species in the solution, producing spurious current that interfered with measurement of the tunneling current. Molecular Imaging Inc., cofounded by Stuart Lindsay, developed an “electrochemical STM” with an integral potentiostat that enabled the STM-sample potentials to be defined relative to the electrochemical potential of the sample, solving this problem. NJ, with others, learned how to insulate STM tips except at the apex of the tip to suppress reactions with electron donors and acceptors in solution.

Armed with these tools, NJ set about pioneering applications of STM and AFM to problems in electrochemistry. His 1996 STM investigation of chemisorbed porphyrins (Figure 2a) on graphite was seminal in terms of opening this field (Figure 2).[87] In an earlier 1995 paper, he

had demonstrated that these porphyrins adsorbed flat, forming close packed and crystalline two-dimensional (2D) layers on a graphite surface that was readily imaged at molecular resolution.[6] The 1996 paper documented the influence of the iron redox center and the electrochemical potential of the surface, which fixed the ratio of Fe(II)/Fe(III) within these monolayers on their apparent height, determined by the conductivity of individual molecules within these monolayers.[87] At a constant tip-sample bias of −100 mV, iron protoporphyrin (FePP) molecules "light up" within mixed monolayers containing PP, producing larger apparent heights (Figure 2d). When the electrochemical potential of the surface is varied across the range about the reversible potential for FePP, $E°$, (Figure 2e), the apparent height shows a maximum at $E° = -0.44$ V *versus* the standard calomel electrode (SCE), the potential at which Fe states are resonant with the tip-sample potential (Figure 2f).[87] These data provided early evidence for electrochemically controlled resonant tunneling in molecular systems,[87] with more detail added by subsequent papers.[2,6,7,88–95] These papers also established that such precise control of the electrochemical potential of the surface was compatible with atomic and molecular resolution imaging.

In some of the earliest *in-situ* investigations of the electrochemical reactivity of molecules, AFM and STM were used in combination and provided complimentary electronic and topographical information.[2,7,95,96] For the electrochemical oxidation of guanine monolayers on graphite,[96] AFM produced lower noise images, documenting the formation of nanometer-scale voids in these monolayers during the oxidation process. The higher resolution of STM images provided an opportunity for changes in the ordering of individual molecules to be observed in some cases,[96,97] but STM images acquired for guanine and adenine monolayers on graphite showed potential-dependent superpositions of the graphite lattice with that of the monolayer.[7] Because an organic monolayer on an electrode surface is located within the electrical double layer, the influence of an electric field operating on the monolayer must also be considered.[98] The thickness of the monolayer and the radius of the adsorbed ions can be as small as a few Ångstroms, thus, the electric field between these two charged layers—the electrode surface and oppositely ions located at the inner Helmholtz plane—can be large and controllable over a broad range (*e.g.*, -10^9 to 10^9 V/m) using the applied electrode potential. These observations provide the basis for the conclusion that the local distribution of electron densities inside of a molecule can be modified and controlled by the electric field.[2,7] Because the local electron distribution of a molecule determines its reactivity, this discovery is significant in understanding or designing electric-field-induced redox reactions, and even chemical reactions.[99–101] For *in situ* investigations focusing on the reactions of molecular monolayers, AFM operating in the recently developed tapping mode was used effectively, in preference to STM, a pervasive trend at this time.[102–106]

As the electrode potential changes, the surface charge density can be continuously changed, reaching values as high as 0.1 electron per surface atom. Another important contribution is the discovery of charge-induced order-disorder transition of an organic monolayer at a solid–liquid interface.[91] Using 2,2'-bipyridine (22'BPY) as an example, he found that the molecules stack into polymeric chains that are randomly oriented on the surface at low charge densities (Figure 3a).[94] Increasing the charge density to a critical value, the polymeric chains are aligned along one of the Au(111) lattice directions in a fashion similar to the isotopic-nematic transitions of liquid crystals (Figure 3b,c).[91,94] The surface-charge-

induced order–disorder phase transition is reversible and this phenomenon is general, existing in other organic molecules such as 4,4'-bipyridine,[94] 1,10'-phenanthroline,[93] and even anions[105] as well as large biomolecules such as lipids.[104]

The surface-charge-induced reversible order–disorder phase transitions of lipid films, providing an explanation of the unusually high diffusion of myoglobin (Mb) in a solid-like lipid film.[104] Similarly, the surface charge induced structural changes of monolayers of phosphate ions, helping understand the unusual electrochemical potential dependence of the electron transfer behavior of cytochrome c.[105] Immobilizing metalloproteins with intact and/or optimized conformations on electrode surfaces is not only important for the study of biological processes, but also integral to the development biosensors and the investigation of biosynthetic processes. However, these molecules often denature upon adsorption onto a solid electrode. These studies were foundational for his development of practical sensors/biosensors, as described below.

QUANTUM TRANSPORT IN ONE-DIMENSIONAL METAL AND CONDUCTIVE POLYMER NANOSTRUCTURES

In the late 1990s, metal quantum point contacts (QPCs) became tools for the investigation of the conductivity of single molecules. These QPCs exhibited quantized conductance in units of G_0 (Eq. 1) were prepared using mechanically controlled break junctions[107–112] and by forming QPCs at a metal surface by using the tip of a scanning tunneling microscope (STM) to contact a metal surface.[12,113,114]

$$G = n2e^2/h = n77.4\,\mu\mathrm{S}, n = 1, 2, 3\ldots \quad [1]$$

Li and Tao demonstrated the first electrochemical formation of a copper metal QPC in an STM in 1998 (Figure 4).[115] In these experiments, a partially insulated STM tip was positioned a few nanometers above a Au(111) surface in an aqueous copper plating solution and copper metal was electrodeposited with the aid of reference and counter electrodes also immersed in this solution (Figure 4a). In this configuration, the deposition of copper and its dissolution from the nanowire could be controlled using the potential applied to the tip (Figure 4b). This configuration provided a means by which the diameter of the copper nanowire could be precisely controlled *in situ*. Measurements of the tip–sample current *versus* time recorded during Cu electrodeposition and subsequent dissolution produced conductivity steps either up (during deposition) or down (during dissolution) in multiples of G_0 (Figure 4c).[115] Conductance histograms for this system, compiled from hundreds of deposition, stripping, and re-deposition traces (Figure 4b) showed prominent peaks at G values predicted by Eq. (1). This 1998 experiment was the direct progenitor of the STM-break junction method[116] that would be applied in 2003 to measurements of the single-molecule conductance.

Analogous experiments with poly(aniline) (PANI) nanowires were less readily interpreted.[15,17,18] Initially, a lithographically fabricated gold nanogap was used, but an STM tip–sample gap was also studied because it facilitated investigations of the influence on conductance of stretching of the PANI nanowire.[15,17,18] Whereas metal QPCs in the STM

showed discrete conductance steps spaced by G_0 as the tip–sample distance was increased by a few Ångströms,[12,113,114] decrementing the conductance of PANI nanojunctions required increasing the tip–sample spacing by many nanometers.[19] Stepped conductance traces acquired while stretching PANI junctions showed steps corresponding to 10^{-7}–10^{-8} S, orders of magnitude smaller than G_0. These conductance steps were not attributed to conductance quantization.[19] Instead, it was hypothesized that they were caused by transitions between polymer chain configurations for the multiple polymer chains present within the tip–sample gap.[19] Conduction through PANI nanowires also varied as a function of its oxidation state. The conductivity of the PANI bridge "telegraphically" alternated between zero and one level for cases where a small amount of PANI was deposited, and between several current levels when larger amounts were deposited.[117] The number of accessible conductivity states could be adjusted by equilibrating the PANI nanowire at various potentials. This discrete conduction behavior was attributed to fluctuations of the polymer between doped, conducting, and undoped insulating redox states.[117] This initial series of experiments on PANI occurred in the 1998–2003 time period, immediately before Tao's group re-focused on understanding the conductivity of smaller organic molecules.

Years later, Tao and colleagues revisited investigations of PANI nanowires in the STM.[14,115,118] The application of tensile stress to these junctions was observed to produce two behaviors: Initial stretching caused an increase in conductivity that was attributed to alignment of polymer chains; with continued stretching, a maximum conductivity was observed, followed by a staircase of declining conductance steps resembling those seen in the copper nanowire system.[115] In 2007, Lindsay and Tao conducted a comprehensive investigation of electrodeposited PANI nanowires in planar, nanofabricated (static) metal gaps immersed in aqueous solution.[14] In these experiments, negative differential resistance, a common feature of single-molecule conduction including studies of aniline oligomers,[118] was observed for PANI systems where a relatively small amount of the polymer had been electrodeposited.[14]

CHEMICAL AND BIOLOGICAL ANALYSIS

Among NJ's first forays into chemical sensing was his development in 1999 of high-resolution SPR.[21,119] This advance was achieved by replacing the commonly used single photodiode with a quadrant photodiode chip, which permitted real-time subtraction of "background" and "active" surface regions and common mode noise reduction caused by light source fluctuations, mechanical vibrations, and thermal drift.[21,119] This high-resolution SPR modality increased the refractive index sensitivity by orders of magnitude, affording a resolution of 10^{-8} refractive index units (RIU) and a response time of 1 μs.[21,119] This level of refractive index sensitivity enabled new and heretofore impossible applications of the SPR. One of these applications involved the detection of adsorbed layers of toxic elements, such as lead[119] and arsenic.[120] In these examples, reference and sample areas of the sensor were coated with an unfunctionalized *n*-alkanethiol self-assembled monolayer (SAM), and a carboxylate (-COOH)-terminated SAM, respectively. Metal cations in a contacting solution phase were bound by the carboxylate-terminated thiol SAM, but not at the unsubstituted SAM.[119,120] The limit of detection for this enhanced SPR technique for Pb^{2+} (40 ppt)[119] and As (as $H_xAsO_4^{(3-x)-}$) was 10 ppb,[120] as required by the United States Environmental

Protection Agency. This technique would form the basis in 2004 of the startup company Biosensing Instruments Inc. (*vide infra*).

At the same time, the Tao group began to investigate applications of conductive polymer nanojunctions to problems in chemical analysis. This new research direction was inspired both by his previous work on STM/conducting polymer conductivity measurements,[14,15,17,18,114,117] and by observations that the quantum conductance of these systems was influenced by molecular properties as well as the electronic structure of the solid state.[16–18] This research thrust was launched by a 2003 paper titled, "A Conducting Polymer Nanojunction Sensor for Glucose Detection,"[121] in which a PANI/poly(acrylic acid) channel bridging two lithographically fabricated metal nanoelectrodes was doped with the enzyme glucose oxidase (GO_x). The detection of glucose by this sensor occurs when GO_x produces H_2O_2 in the presence of glucose, oxidizing the PANI and enhancing its electrical conductivity.[121] The nanoscale dimensionality of the sensor made possible a rapid (200 ms) response time for glucose detection.[121] This paper showed that nanojunctions, previously the domain of physicists, provided analytical chemists with a new and versatile tool for designing chemical sensors.

An unexpected advantage of such nanojunction nanosensors is their ability to operate in unprocessed, real samples. Inspired by Justin Gooding's work on peptides,[122] a conducting polymer nanojunction sensor for the detection of heavy metals in drinking water was developed,[123] followed by a conducting polymer nanojunction breath sensor, that detected ammonia at parts-per-billion levels.[124] Elsewhere, several groups reported on the amazing sensitivity and other overall properties of nanosensors.[125–127] Taking inspiration from this work, in 2004, NJ and Larry Nagahara of Motorola Labs decided to explore the properties of low-dimensional carbon materials in sensors. The capability of Motorola to create silicon-based chips with 1 or 2 single-wall carbon nanotubes (CNTs) in a micron-scale gap enabled modification of the CNTs, leading to the demonstration of ultra-low parts-per-trillion level sensing of heavy metal ions[128] and pM level detection of viral RNA strands for Hepatitis C.[129] The sensitivity of the latter would eliminate the need for amplification by polymerase chain reaction, PCR, of RNA strands, a requirement of many current methods used for virus detection.

The versatility of PANI nanojunction sensors was demonstrated in 2007 with the operation of these sensors both in conductometric and amperometric modes (Figure 5a,b).[34] Conductometric detection is obtained by transducing the channel conductance, just as in chemical field-effect transistors (FETs). Amperometric detection exploits the direct oxidation/reduction of a target molecule at the PANI channel (Figure 5c). Nanojunction sensors can be operated in either of these modes, or in both simultaneously (Figure 5d). The attributes of these two modes were compared for the detection of the neurotransmitter dopamine.[34] The work came to fruition with the selective detection of dopamine in the presence of 1000-fold excesses of an interferent, ascorbic acid.[34,130,131] Versions of this technology were commercialized for the detection of exhaled nitric oxide,[132–134] an airway inflammation biomarker, and for the ultrasensitive detection of explosives.[135,136]

In 2000–2004, NJ's team was also undertaking chemical analyses of gases using inexpensive quartz crystal resonator tuning forks, typically used in electronics and watches for timing. Tuning forks could be repurposed as sensitive mass measurement transducers for chemical sensing.[137–141] Working with Motorola scientists Larry Nagahara and Ray Tsui, NJ's team created an alcohol sensor embedded in a cell phone. In this device, a polymer nano/microwire composite sensing material bridged between the prongs of the tuning fork. This system later evolved to become a wearable mobile sensor for measuring the mechanical properties of light-sensitive materials[142] and for the spatial-temporal tracking of exposure to pollutants[134,143–146] and particles.[147] The latter systems were introduced to the public by Dr. Francis Collins, Director of the National Institutes of Health, in the 2015 (Mobile) *mHealth Summit* in Washington, D. C.

In 2009–2010, aware of the fabrication limitations of silicon-based sensors and the relatively high cost of maintenance of clean room operations, NJ sought a relatively inexpensive way to create sensors. Inspired by the work of Ken Suslick on colorimetric sensor arrays,[148] NJ and Erica Forzani began the search for sensing applications with high market demand and created a sensor array for selective detection of oxygen and carbon dioxide in breath, enabling them to measure energy expenditure (kcal/day) *via* indirect calorimetry.[149–151] This innovation later led to several practical applications to improve the efficacy of weight and disease management in overweight and diabetic patients[152] as well as exercise practices,[153] and to spin off the second of NJ's start-up companies, TF Health Co. (*vide infra*).

In 2008, NJ was named Director of the Center of Bioelectronics and Biosensors at The Biodesign Institute, Arizona State University, which has ~30 permanent researchers and over 20 institutional collaborators, such as Banner Neurological Institute and The Mayo Clinic. Under his leadership, the Center's scientific contributions expanded in new directions including the fields of chemical and physical sensors for noninvasive environmental sensing[154–158] and medical applications.[159,160]

ELECTRICAL CONDUCTANCE OF SINGLE MOLECULES

A long-standing objective in the subfield of molecular electronics has been to develop molecular devices that will complement—and eventually even supersede—current semiconductor-based technologies.[161–163] NJ Tao's flagship research in molecular electronics, especially in molecular transport junctions (MTJs), established his as a leading group in this area. In 2003, Tao and one of his students invented the scanning tunneling microscope break junction (STM-BJ) method, possibly his most impactful contribution to molecular electronics.[116] The STM-BJ method and its variants have been adopted as a standard measurement protocols for the investigation of electron transport in single molecules.

Although a number of methods had been developed to measure the charge transport through single molecules by 2003, the main problems with measurement were creating the electrode–molecule–electrode junction in a reproducible way and handling the inevitable variability in the properties of single molecules. The STM-BJ method starts with repeatedly driving a conducting STM tip into contact with and then pulling away from an Au (111)

surface coated with molecules containing anchoring groups that can bond to Au; the conductance curves of the whole processes are simultaneously recorded. As shown in Figure 6a–A, at the start of the STM tip pulling, Au quantum contacts were formed, as evidenced by the conductance steps at multiple integers of the conductance quantum (Eq. 1). Remarkably, after the breaking of the of the quantum contacts, molecules were contacted with the tip and the substrate to form an Au-molecule(4,4'-bipyridine)–Au junction, as indicated by the conductance steps being 100 times smaller than the conductance quantum (Figure 6a–C). No conductance steps were observed in the molecule conductance window when no molecules were applied. In this method, the reliability issue was successfully resolved by forming and measuring the junctions thousands of times. The conductance histogram (Figure 6a–B,D,F) shows statistically significant results that capture the inherent variability of single-molecule measurements.

As soon as single molecule STM-BJ conductance data were available, it was apparent that Eq. [1] was insufficient to describe these data. A molecular junction is a hybrid system that exhibits a conductance, G, determined by both the molecule and the molecule–electrode contacts:

$$G = \frac{n2e^2}{h}\frac{\Gamma^2}{\Delta^2 + \Gamma^2} \quad n = 1, 2, 3\ldots \qquad [2]$$

where Γ and Δ= $E - \varepsilon$ are the coupling between molecule and electrode, and the energy difference between the conduction orbital and the Fermi level of the metal electrodes respectively.[162] To account for differences in the electrode–molecule contact and to confirm the formation of Au–amine and Au–thiol bonds, a follow-up study was carried out that simultaneously measured the conductance and breakdown forces of the molecule junctions.[39] The breakdown force of the Au–thiol contact was found to be *ca.* 1.5 nN (Figure 6b) whereas that of the Au–amine contact was *ca.* 0.7 nN, in agreement with theoretical calculations.

Soon after the discovery of STM-BJ, two seminal publications based on this technique were published from other research groups. The first, by Reddy *et al.*, reported the measurement of single-molecule Seebeck coefficients $S_{junction}$ for 1,4-benzenedithiol (BDT), 4,4′-dibenzenedithiol, and 4,4′-tribenzenedithiol, revealing a molecular length dependence on the value of $S_{junction}$.[164] The second, by Venkataraman *et al.*, reported an investigation of seven biphenyl molecules with varying ring substitutions that imparted a twist angle to these molecules.[165] The single molecule conductance of these molecules decreased as the twist angle increased,[165] quantitively in accord with theory.[166] These two investigations enabled by STM-BJ are cornerstones in the development of the field of molecular electronics.[167,168] Subsequent development of STM-BJ by the Tao group enabled the capture of fast events (~1 ns) by using high-speed electronics (Figure 6c),[12] observations of the effects of anchoring groups,[169] the introduction of target-molecule-specific binding sites, assessments of the quantitative influence of molecular geometry,[170] and the elucidation of the origin of some junction instabilities,[40] making STM-BJ a comprehensive experimental platform in measuring various single-molecule transport properties.

A review of NJ's expansive contributions to molecular electronics is beyond the scope of this Perspective, but several especially impactful contributions are described. One of these is the gating of electron transport in molecular junctions using an electrochemical gate, which contributed to an understanding of electron transport mechanisms in molecular junctions and enabled device applications. In fact, a number of gating modalities were explored (Figure 7).

One such gating modality involved mechanical control of the STM tip–surface spacing. The influence of tip position on the apparent conductance was noticed by Haiss *et al.* who reported that the conductance of a molecule located in the gap between an STM tip and the surface oscillated between two discrete values as the molecule spontaneously connected and disconnected from the STM circuit.[171,172] NJ termed this behavior "blinking."[173] Blinking did not occur when the tip–surface distance exceeded the length of the molecule under examination, and this parameter could also be used to control the angle of a molecule within the gap, thereby affecting the conductivity.[171,172] With ac modulation on the tip–surface distance, NJ was able to distinguish in real time between an open gap, which produced large current modulations, and a molecular junction, which showed damped current modulations. Simultaneous measurement of the conductance of the gap was facilitated as well.[173] A "blink and pull" method[174] took this experiment one step further, by probing the ac conductance while the tip–sample distance was increased, causing the tilt of a single molecule to be reduced. This technique enabled precise measurement of conductance as a function of molecular tilt,[174] exceeding what had been possible in previous studies. These papers established that precise mechanical control of single-molecule conductance was achievable and understandable at a fundamental level.[173,174]

Although rectification should not be termed "gating", it is a phenomenon of interest in molecular electronics. Single-molecule rectifiers based upon asymmetric organic molecules were predicted in the 1974 paper by Aviram and Ratner.[163] The concept was experimentally demonstrated for asymmetric single molecules in self-assembled monolayers by Luping Yu and coworkers.[175] Isolated single molecular diodes were achieved in 2005 by Elbing *et al.* [176] using a mechanically controllable break junction. However, switching of the forward-biased direction for the diode, dictated by the molecular orientation in the junction, was not possible in this case. Using an asymmetric diblock dipyrimidinyldiphenyl molecule, NJ demonstrated this capability in 2009 using the STM-BJ blinking methodology, which enabled an immobilized molecule to be expelled from the junction and a new molecule (or the same one) reattached with reversal of its polarity.[177]

Mechanical gating was also achieved by the application of tensile and compressive stressed to single molecules. This discovery in 2012 involved the modulation of the conductance of 1,4'-benzenedithiol (BDT) molecules by applying either a tensile stress or a compressive stress to the molecule using the STM tip.[178] The conductance of BDT was perturbed by up to an order of magnitude by these forces. Counter to intuition, in these experiments the BDT conductance was enhanced during stretching and depressed during compression. The HOMO of the BDT migrates toward the Fermi level of the Au electrodes during stretching, closer to resonance with the Fermi energy of the Au contacts.[178]

Related to transport gating in molecular junctions is the issue of heating.[179,180] NJ and his students studied this issue for 1,8'-octadecanedithiol using the STM-BJ technique.[181,182] These experiments afforded an estimate of the temperature increase induced by current flow of ~30 K for V_{bias} = 1.0 V, the highest bias for which these junctions were stable.[182] Subsequently, more detailed STM-BJ studies of C6, C8, and C10 alkanedithiols revealed that heating of these molecules increased with decreasing molecular length; these junctions showed complex bias dependences in which maximum heating of these molecular junctions was seen at $V_{bias} \approx 0.80$ V, because at higher V_{bias} electron–electron cooling occurs in accord with the recently proposed hydrodynamic theory proposed by D'Agosta and Di Ventra.[183]

Electrochemical gating of molecular junctions was demonstrated by NJ and his group in 2005, in a flurry of papers describing an electrochemically gated single-molecule FET,[184] electromechanically controlled conductance switching,[185] and electromechanically controlled negative differential resistance-like (NDR-like) behavior.[186] But there would be many more publications from NJ and his students exploring this phenomenon, reporting redox-gated electron transport in electrically wired ferrocene molecules,[187] and electrochemical control of electron transport in graphene[188] and in coronenes.[189] Furthermore, electrochemically gated single-molecular switches[190] and ambipolar single-molecule FETs[191] were successfully demonstrated, pushing single-molecular device applications a step forward. Using temperature control as the thermal gating, Tao and his group also investigated electron transport in single redox molecules,[192] the electron–phonon interactions in single-molecular junctions,[193,194] tunneling-to-hopping transitions in single-molecular junctions,[195] low-bias rectification in a single-molecule diode,[196] thermopower and transition voltages,[197] and the nonexponential length dependence of conductance.[198] Lastly, the Tao group measured the electronic spin filtering capability of a single chiral helical peptide by using a ferromagnetic electrode source to inject spin-polarized electrons.[199]

What might NJ have done next in this area? Based upon the collective experience of the authors, most of whom worked with him over many years, one goal that he articulated was to extend the measurement platform to explore and to control chemical reactions at the single-molecule level, including the development of the ability to determine subtle molecular structural information, such as the determination of chirality for two stereoisomers. A second aspiration was to integrate optical imaging techniques with STM-BJ to explore the coupling between electronic transport and light in single-molecule junctions, work that would have impacted both molecular electronics and molecular plasmonics.

CHARGE TRANSPORT IN SINGLE DNA MOLECULES

Beyond its role as the carrier of genetic information, DNA has become an important material in nanoscience and nanotechnology.[200] The properties of DNA, including self-assembly, programmable structural control, rich chemistry provided by the polymer backbone with varying side groups, and controllable helical structure, have led to a wide variety of innovations utilizing DNA as a structural, mechanical, lithographic, or biotechnology element.[201–205] However, the utilization of DNA as a circuit element has proven difficult

due to its complex electronic structure and the strong interplay between the electronic and structural degrees of freedom. Much of our understanding about the utility of DNA as an electronic element has come from Tao's work, and the work he inspired.

After the development of the STM-BJ methodology in 2003,[206] NJ's attention returned to a topic that had interested him since his Ph.D. studies: the properties and dynamics of DNA.[76,77,207] This time, however, he placed the emphasis on the electronic properties of DNA. This was an opportune time for such studies as there was significant conflict in the field about the inherent charge transport properties of DNA. Reports emerged that ran the gamut of possible electronic capabilities for DNA including insulating,[208,209] semiconducting,[210] conducting,[211] and proximity-induced superconductivity.[212] The incongruity in conductance studies was mirrored by the significant disparity in charge-transfer properties seen in photochemical and electrochemical measurements.[213–216]

Tao's background in electrochemical STM[217] and the advent of the new break junction system[206] gave a unique opportunity to begin addressing these issues: The DNA duplexes could be measured in aqueous environments that could help preserve the inherent DNA structure, which may be lost if measuring the DNA in ambient conditions or vacuum as had been done in some other experiments. Initial experiments on short DNA duplexes (< 18 bp) showed that G:C repeat sequences yielded a conductance proportional to the length of the sequence, indicating hopping, whereas A:T pairs inserted into the stack yielded a weak exponential, suggesting that the charges tunneled through the A:T barriers.[218] This work placed conductance measurements for short sequences in line with photochemical measurements with similar outcomes.[50,214,219,220] Interestingly, however, the temperature dependence could not be determined within the temperature window of the experiment (between the liquid freezing temperature and the DNA melting temperature), which left the opportunity open for more complex transport behavior.[45,221]

Over the next 15 years, a variety of work from Tao and many others placed intensive focus on understanding the native electronic behavior of DNA duplexes,[222–229] RNA:DNA hybrids,[230] and G-quadruplexes.[231–233] NJ's group focused on understanding the thermal, mechanical, and thermoelectric properties of these systems, and how these properties relate to the electronic structure.[234–237] The thermoelectric measurements demonstrated conclusively that DNA transport was hole dominated: hopping-dominated in G:C rich systems, and tunneling dominated through short A:T bridges, but it again transitioned to hopping if the A:T bridge became long enough.[237] The addition of the Seebeck coefficient to the conductance measurements for these systems provided a second methodology to verify previous results from conductance and the resulting implications about the transport. These measurements heralded new opportunities for quantifying contact properties and understanding alignment of energy levels between bases in the stack.

Tao's group made important advances in understanding the contact and coupling properties within DNA and their influence on conductance by utilizing the pulling capabilities of the STM-BJ system on duplexes of various designs.[234–236] These results demonstrated that when pulling on the molecule, conductance breaks down once the hydrogen bonds in the first one or two bases break, which means the forces must be carefully controlled in DNA to

observe conductance behavior. This result helps rationalize the wide variety of initial conductance values observed in DNA-based systems. An additional mechanical approach was to apply a small AC modulation to the tip (~1–2 Å) at a higher frequency (2 kHz).[173,234,238] This approach enables more direct information to be determined about the coupling between bases, especially purines, in the base-stack. This advance led to understanding of the effects of coupling between bases in the stack when placed in interstrand or intrastrand configurations, which has helped lead to designs for improving the conductance of DNA-based structures.

The experiments described above indicate that careful design of DNA sequence and structure could lead to unique effects, but they also indicate that obtaining significant changes in the overall conductance or modulating the transport properties of DNA will require additional changes to its chemical and electronic properties. In 2015, Tao's group demonstrated that in G:C rich hopping systems, the coherence length of the charge carriers (holes) could extend beyond a single guanine base.[239] This finding was followed with another study in collaboration with Beratan's group that began to provide design rules for engineering the coherence and coupling between bases.[240] These studies were quickly followed by other groups demonstrating longer coherence lengths in DNA, RNA, and peptide nucleic acid (PNA) systems than initially expected from length-dependent conductance measurements,[44,230,241–243] which may in the long term provide a basis for the rational design of DNA-based devices.

Developing devices is one of the ultimate goals for DNA transport studies. For native structures, the devices will likely be sensor systems, and Tao's group conducted initial studies to show the impact of single-base mismatches[244] and epigenetic effects[245] on conductance, which have been expanded on by other groups.[246–248] Beyond these native structures and sequences, focus has been given to other device designs as well, such as the creation of a G-quadraplex-based current-splitting element,[232] which may give way to 3-terminal devices or advanced wiring concepts for electronic devices (Figure 8). Inclusion of non-native bases,[249] intercalators,[250] and metal ions[251] could be used to create DNA-based wires,[252] transistors,[249] diodes,[253] or photoactive elements.

Single-molecule transport experiments have dramatically advanced our understanding of charge transport in DNA. These data and the deeper understanding enabled by it have powered the nascent field of DNA-based device design, spawning proof-of-principle systems for sensing and electronic circuit elements, including current-splitting and potential 3-terminal elements,[232] diodes,[254] and systems that support long-range transport over tens of nanometers.[231] Moving forward, the initial experiments on the length coherence of carriers in systems may lead to new designs that harness the quantum properties of DNA's electronic structure. These innovations could result in both new sensing paradigms where changes in sequence result in modifications of coherence and new devices that engineer interference effects or modifications to the electronic structure for device applications.

Much is yet to be learned, including developing methods to engineer and to control the coherence length in these materials, developing new avenues for integrating these devices into larger scale structures and the outside world, fundamental knowledge about how to align

and to manipulate the energy levels in DNA in a robust and reliable way, and understanding how fluctuations and the inherent flexibility in these systems contribute to the electronic properties and how these properties can be utilized for improvement. The knowledge gained from Tao's experimental insights over the years built an important foundation for exploring these areas, impacting not only the field of DNA-based electronics but research across nanosystems, where emerging technologies such as DNA-based memories and computing,[255] origami-enabled electronic design,[256] and long-range transport in protein-based systems[257] continue to gain momentum.

OPTICAL MICROSCOPY AND DETECTION TECHNOLOGIES

Optical microscopy is one of the most common and powerful tools used in materials and life sciences research labs. Advances in microscopic imaging technologies have played critical roles in biomedical research and clinical applications.[258–260] A large portion of NJ Tao's research career was devoted to the development of new functional imaging tools for chemical and biological applications. His group invented two groundbreaking microscopy technologies for functional imaging of chemical and biological targets.

The first imaging technology is a multifunctional plasmonic-based electrochemical impedance microscopy (P-EIM),[23,261,262] integrating surface plasmon resonance microscopy (SPRM)[28,263,264] and electrochemical impedance microscopy (EIM)[25] into a conventional inverted microscope (Figure 9). Unlike conventional electrochemical impedance spectroscopy,[265] which measures alternate current amplitudes, P-EIM exploits the more sensitive optical detection of surface plasmonic signals for metals on the surface charge density,[25] thus enabling fast (sub-ms) and noninvasive imaging of impedance at near diffraction-limited resolution without an electrode array or a scanning probe. In addition, P-EIM maps the local electrical polarizability and conductivity, which reflects local changes in the cellular structure and ionic distribution. Compared to conventional optical imaging techniques, the plasmonics-based approach can image not only the morphology, but also molecular binding events and local chemical information taking place at fast time scales. Important benefits of this approach include fast, noninvasive, and quantitative imaging of optical mass change, electrochemical current, and impedance of various samples, from small molecules to whole cells.

A variety of applications for the P-EIM technology have been demonstrated, including trace chemical analyses (Figure 10);[23] catalytic reactions[266–270] and thermal diffusion[271] of nanomaterials; charge distributions in 2D materials;[63] detection of single DNA,[69] exosomes,[272] or single virus (Figure 11);[28] tracking single organelle transportation in cells;[273] time-resolved digital immunoassay;[274] nano-oscillators for detection of charge,[275] molecules,[276] and biochemical reactions;[277] ligand–membrane protein interactions in intact cells;[261,278–283] tracking bacterial metabolic changes for antimicrobial susceptibility tests;[284] and mapping action potentials in single neurons (Figure 12).[285] With further improvement of this technology, particularly in signal-to-noise ratio, P-EIM could lead to label-free functional detection of single proteins. This purpose was a goal of NJ's since 2000, when he calculated that, with sufficient light, SPR was capable of detecting single protein molecules (as noted during discussions with Dr. Shaopeng Wang, then his postdoc at FIU).

The second imaging technology developed in the Tao group is mechanically amplified detection of molecular interactions (MADMI).[286,287] Measuring molecular binding to membrane proteins is critical for understanding cellular functions, validating biomarkers, and screening drugs.[288,289] Despite its importance, measuring small molecule binding to membrane proteins in their native cellular environment remains a challenge.[276,278,279] However, MADMI can measure the mechanical deformation in cell membranes that accompanies the binding of molecules with the membrane proteins on the cell surface. The laws of thermodynamics predict that when molecules bind to a surface, the surface tension changes. According to thermodynamics, the surface concentration (Γ) of molecules bound on the membrane surface is given by:[286]

$$\Gamma = -\frac{d\gamma}{RTd(\ln c)}, \quad [3]$$

which applies to ideal solutions at a constant temperature and pressure, where γ is the surface tension, R is the gas constant, T is temperature, and c is the bulk analyte concentration. $RTd(\ln c)$ is the chemical potential of the molecules. From Eq. (3), molecular binding is proportional to the surface tension change. Because cells are soft, a small change in the surface tension can induce a substantial mechanical deformation of the cell, leading to signal amplification. Therefore, the interactions of molecules with membrane proteins on a cell can be measured by determining the mechanical deformation of the cell membrane. Because the signal does not scale with the size of analyte molecules, MADMI is particularly suitable for quantifying the binding kinetics between small molecule drugs and membrane protein targets in their native environment. Quantification of binding kinetics between protein, peptide, and small-molecule ligands on different classes of membrane proteins on adherent[286] and floating cells[287] has been demonstrated. Further development of MADMI for improved sensitivity, higher multiplexing capabilities, automated deformation-tracking algorithms, and testing in wider ranges of cells and ligands will lead to label-free biomarkers and drug-discovery tools for cell-based membrane protein binding kinetic studies.

To detect minute, nanometer-scale membrane deformations accurately, Tao's lab developed a differential detection algorithm for tracking the edge movement of a cell using optical imaging (Figure 13). The method nulls common-mode noise in the optical system, thus achieving superior detection limits. This image-based differential tracking method not only works for detection of molecular interactions, but has also been adapted for broader applications, including tracking fast cellular membrane dynamics;[290] tracking nanometer-scale cellular membrane deformation associated with single vesicle release;[291] determining electrochemical surface stress of single nanowires;[292] performing charge-sensitive optical detection of molecular interactions;[62,64] and measuring subnanometer mechanical motion accompanying action potential in neurons, where the detection limit was further improved *via* signal modulation and digital filtering.[293] This differential tracking method is extremely general and is expected to have a range of applications in phenomena for which nanoscale mechanical deformations are important.

TRANSLATING SCIENCE TO SOCIETAL BENEFIT BY COMMERCIALIZATION

NJ was a successful entrepreneur as well as a scientist. Upon his return to ASU from Florida International University in 2004, he founded Biosensing Instrument Inc. (BII) with Dr. Tianwei Jing and Professor Feimeng Zhou of California State University, Los Angeles. From its inception, NJ was actively engaged in BII, spearheading product design, identifying applications, and even providing customer support. After just one year of development effort, BII sold its first unit to the University of Texas at Austin for gas-phase applications. BII grew quickly and diversified its product line to include fully automated, multichannel SPR instruments and microscope-based variants, along with various analysis modules for diverse fields, including surface chemistry, single-cell analysis, and studies of cancer and neurological disorders, to integration with other analytical techniques for the detection of species of biological, pharmaceutical, and environmental importance. The companies' record of innovation and commercialization has been recognized by two recent R&D 100 Awards.

As NJ's research group attained momentum in chemical and biological sensing in the 2003–2008 time frame, the resulting technologies presented further opportunities for commercialization. In 2008, NJ and Erica Forzani co-founded TF Sensors LCC, which soon became TF Health Corp. with the aim of developing sensors for health monitoring. The addition of two scientists to the TF Health team, Drs. Francis Tsow and Xiaojun Xian enabled a series of product developments starting in 2011 with indoor air quality sensors compliant with the Centers for Disease Control and Prevention guidelines (Figure 14). In 2012, a sensor for the analysis of exhaled nitric oxide in asthma patients was introduced. And in 2013, a wireless metabolism tracker, Breezing, was demonstrated (Figure 15). This product, highlighted by the BBC,[294] Forbes,[295] and Scientific American,[296] was a commercial success and received numerous awards and recognitions, including the Materials Research Society's iMatsci, Consumer Technology Association's 2017 Baby Tech Awards finalist, the Flinn Foundation Entrepreneur Award, and Arizona Commerce Authority's Challenge. Refinement of the Breezing platform has culminating in the demonstration of an innovative smart mask device (Breezing Pro) that provides data that dieticians can use to provide precise nutritional and exercise advice to their clients (for more details see: https://breezing.com/resources/).

CONCLUSIONS AND OUTLOOK

Electrochemistry, molecular electronics, surface science, and chemical sensing were all impacted by the tremendous reach of NJ's research over more than 30 years. In spite of its diversity, a common thread running through all of NJ's science is an emphasis on applying simple physical principles, and asking simple questions based upon these principles, as a means for understanding complex phenomena. He applied this reductionist strategy successfully in all of the areas he investigated.

Now, with his prior work as a foundation, we are left to consider where each of these areas will progress: What are the frontiers in metabolic sensing, molecular electronics, DNA-based electronic devices, and optical microscopy and detection that could be advanced, or

simplified using novel physical apparatuses? What questions could be answered by looking across these domains? In this Perspective, the goal has been to highlight some of the most exciting science in each of these areas. The new challenge is to apply the understanding generated by NJ's work, along with that of many others over the past 25 years, to answer problems in fields *other than* molecular electronics, surface science, and electrochemistry. This challenge is in the hands of a new generation of scientists, including NJ's many students and postdocs who trained with him and who will pursue this goal, with his inimitable style.

ACKNOWLEDGMENTS:

BX acknowledges financial support by the National Science Foundation under Grant ECCS 2010875. HH acknowledges financial support by the National Science Foundation under Grant DMR-1742807. JH acknowledges financial support from the NSF/SRC SemiSynBio program 1807555/2836. RMP acknowledges financial support by the National Science Foundation under NSF CBET-1803314. SW acknowledges financial support from the National Institutes of Health (R01GM107165, R01GM124335, R33CA202834 and R44GM126720).

REFERENCES

(1). Hihath J; Lindsay S Nongjian Tao (1963–2020). Nat. Nanotechnol 2020, 15, 41565.

(2). Tao NJ; Shi Z Potential Induced Changes in the Electronic States of Monolayer Guanine on Graphite in NaCl Solution. Surf. Sci 1994, 301, L217–L223.

(3). Lindsay SM; Tao NJ; DeRose JA; Oden PI; Lyubchenko YuL; Harrington RE; Shlyakhtenko L Potentiostatic Deposition of DNA for Scanning Probe Microscopy. Biophys. J 1992, 61, 1570–1584. [PubMed: 1617139]

(4). Tao NJ; DeRose JA; Lindsay SM Self-Assembly of Molecular Superstructures Studied by *In Situ* Scanning Tunneling Microscopy - DNA Bases on Au(111). J. Phys. Chem 1993, 97, 910–919.

(5). Tao N Spectroscopic Applications of STM and AFM in Electrochemistry. In Encyclopedia of Electrochemistry; 2003.

(6). Tao NJ; Cardenas G; Cunha F; Shi Z *In Situ* STM and AFM Study of Protoporphyrin and Iron(III) and Zinc(II) Protoporphyrins Adsorbed on Graphite in Aqueous Solutions. Langmuir 1995, 11, 4445–4448.

(7). Tao NJ; Shi Z Monolayer Guanine and Adenine on Graphite in NaCl Solution: A Comparative STM and AFM Study. J. Phys. Chem 1994, 98, 1464–1471.

(8). Tao NJ; Shi Z Real-Time STM/AFM Study of Electron Transfer Reactions of an Organic Molecule: Xanthine at the Graphite-Water Interface. Surf. Sci 1994, 321, 0–7.

(9). Duong B; Arechabaleta R; Tao N *In Situ* AFM/STM Characterization of Porphyrin Electrode Films for Electrochemical Detection of Neurotransmitters. J. Electroanal. Chem 1998, 447, 63–69.

(10). Li CZ; He HX; Tao NJ Quantized Tunneling Current in the Metallic Nanogaps Formed by Electrodeposition and Etching. Appl. Phys. Lett 2000, 77, 3995–3997.

(11). Tao N Electrochemical Fabrication of Metallic Quantum Wires. J. Chem. Educ 2005.

(12). Guo S; Hihath J; Tao N Breakdown of Atomic-Sized Metallic Contacts Measured on Nanosecond Scale. Nano Lett 2011, 11, 927–933. [PubMed: 21294524]

(13). He H; Zhao Y; Xu B; Tao N Electrochemical Potential Controlled Electron Transport in Conducting Polymer Nanowires. Proc. - Electrochem. Soc 2001.

(14). He J; Forzani ES; Nagahara LA; Tao N; Lindsay S Charge Transport in Mesoscopic Conducting Polymer Wires. J. Phys. Condens. Matter 2008, 20, 374120. [PubMed: 21694427]

(15). He HX; Li CZ; Tao NJ Conductance of Polymer Nanowires Fabricated by a Combined Electrodeposition and Mechanical Break Junction Method. Appl. Phys. Lett 2001.

(16). He HX; Li CZ; Tao NJ Conductance of Polymer Nanowires Fabricated by a Combined Electrodeposition and Mechanical Break Junction Method. Appl. Phys. Lett 2001, 78, 811–813.

(17). He H; Zhu J; Tao NJ; Nagahara LA; Amlani I; Tsui R A Conducting Polymer Nanojunction Switch. J. Am. Chem. Soc 2001, 123, 7730–7731. [PubMed: 11481008]

(18). He HX; Li XL; Tao NJ; Nagahara LA; Amlani I; Tsui R Discrete Conductance Switching in Conducting Polymer Wires. Phys. Rev. B 2003, 68.

(19). He HX; Li CZ; Tao NJ Conductance of Polymer Nanowires Fabricated by a Combined Electrodeposition and Mechanical Break Junction Method. Appl. Phys. Lett 2001, 78, 811–813.

(20). Wang S; Boussaad S; Tao N Surface Plasmon Resonance Spectroscopy: Applications to Protein Adsorption and Electrochemistry, Surfactant Science Seriesw; 2003, 213.

(21). Tao NJ; Boussaad S; Huang WL; Arechabaleta RA; D'Agnese J High Resolution Surface Plasmon Resonance Spectroscopy. Rev. Sci. Instrum 1999, 70, 4656–4660.

(22). Yao X; Wang J; Zhou F; Wang J; Tao N Quantification of Redox-Induced Thickness Changes of 11-Ferrocenylundecanethiol Self-Assembled Monolayers by Electrochemical Surface Plasmon Resonance. J. Phys. Chem. B 2004, 108, 7206–7212.

(23). Shan X; Patel U; Wang S; Iglesias R; Tao N Imaging Local Electrochemical Current *via* Surface Plasmon Resonance. Science 2010, 327, 1363–1366. [PubMed: 20223983]

(24). Foley KJ; Forzani ES; Joshi L; Tao N Detection of Lectin–Glycan Interaction Using High Resolution Surface Plasmon Resonance. Analyst 2008, 133, 744. [PubMed: 18493673]

(25). Foley KJ; Shan X; Tao NJ Surface Impedance Imaging Technique. Anal. Chem 2008, 80, 5146–5151. [PubMed: 18484741]

(26). Wang S; Shan X; Patel U; Huang X; Lu J; Li J; Tao N Label-Free Imaging, Detection, and Mass Measurement of Single Viruses by Surface Plasmon Resonance. Proc. Natl. Acad. Sci 2010, 107, 16028–16032. [PubMed: 20798340]

(27). Foley KJ; Xiaonan Shan; Tao N Detecting Molecules Using a Surface Impedance Imaging Technique In 2009 IEEE/NIH Life Science Systems and Applications Workshop; IEEE, 2009; pp 156–158.

(28). Wang S; Shan X; Patel U; Huang X; Lu J; Li J; Tao N Label-Free Imaging, Detection, and Mass Measurement of Single Viruses by Surface Plasmon Resonance. Proc. Natl. Acad. Sci 2010, 107, 16028–16032. [PubMed: 20798340]

(29). Huang X; Wang S; Shan X; Chang X; Tao N Flow-through Electrochemical Surface Plasmon Resonance: Detection of Intermediate Reaction Products. J. Electroanal. Chem 2010, 649, 37–41.

(30). Wang S; Huang X; Shan X; Foley KJ; Tao N Electrochemical Surface Plasmon Resonance: Basic Formalism and Experimental Validation. Anal. Chem 2010, 82, 935–941. [PubMed: 20047281]

(31). Shan X; Foley KJ; Tao N A Label-Free Optical Detection Method for Biosensors and Microfluidics. Appl. Phys. Lett 2008, 92, 133901.

(32). Wang S; Boussaad S; Tao NJ Surface Plasmon Resonance Spectroscopy: Applications in Protein Adsorption and Electrochemistry. In Surfactant Science Series; 2003; p 213.

(33). Aguilar AD; Forzani ES; Leright M; Tsow F; Cagan A; Iglesias RA; Nagahara LA; Amlani I; Tsui R; Tao NJ A Hybrid Nanosensor for TNT Vapor Detection. Nano Lett 2010, 10, 380–384. [PubMed: 20041699]

(34). Forzani ES; Li X; Tao N Hybrid Amperometric and Conductometric Chemical Sensor Based on Conducting Polymer Nanojunctions. Anal. Chem 2007, 79, 5217–5224. [PubMed: 17563117]

(35). Aguilar ADDD; Forzani ES; Nagahara LA; Amlani I; Tsui R; Tao NJ A Breath Ammonia Sensor Based on Conducting Polymer Nanojunctions. IEEE Sens. J 2008, 8, 269–273.

(36). Huang Z; Xu B; Chen Y; Di Ventra M; Tao N; Huang; Xu; Chen; Di Ventra M; Tao. Measurement of Current-Induced Local Heating in a Single Molecule Junction. Nano Lett 2006, 6, 1240–1244. [PubMed: 16771587]

(37). He J; Sankey O; Lee M; Tao N; Li X; Lindsay S Measuring Single Molecule Conductance with Break Junctions. Faraday Discuss 2006, 131, 145–154. [PubMed: 16512369]

(38). Tian J-H; Liu B; Li; Yang Z-L; Ren B; Wu S-T; Tao; Tian Z-Q Study of Molecular Junctions with a Combined Surface-Enhanced Raman and Mechanically Controllable Break Junction Method. J. Am. Chem. Soc 2006, 128, 14748–14749. [PubMed: 17105252]

(39). Xu B; Xiao X; Tao NJ Measurements of Single-Molecule Electromechanical Properties. J. Am. Chem. Soc 2003, 125, 16164–16165. [PubMed: 14692738]

(40). Huang; Chen F; Bennett PA; Tao. Single Molecule Junctions Formed via Au-Thiol Contact: Stability and Breakdown Mechanism. J. Am. Chem. Soc 2007, 129, 13225–13231. [PubMed: 17915870]

(41). Hihath J; Xu B; Zhang P; Tao N Study of Single-Nucleotide Polymorphisms by Means of Electrical Conductance Measurements. Proc. Natl. Acad. Sci 2005, 102, 16979–16983. [PubMed: 16284253]

(42). Xia JL; Diez-Perez I; Tao NJ Electron Transport in Single Molecules Measured by a Distance-Modulation Assisted Break Junction Method. Nano Lett 2008, 8, 1960–1964. [PubMed: 18543978]

(43). Liu C; Xiang L; Zhang Y; Zhang P; Beratan DN; Li Y; Tao N Engineering Nanometre-Scale Coherence in Soft Matter. Nat. Chem 2016, 8, 941–945. [PubMed: 27657870]

(44). Beall E; Ulku S; Liu C; Wierzbinski E; Zhang Y; Bae Y; Zhang P; Achim C; Beratan DN; Waldeck DH Effects of the Backbone and Chemical Linker on the Molecular Conductance of Nucleic Acid Duplexes. J. Am. Chem. Soc 2017, 139, 6726–6735. [PubMed: 28434220]

(45). Hihath J; Chen F; Zhang P; Tao N Thermal and Electrochemical Gate Effects on DNA Conductance. J. Phys. Condens. Matter 2007, 19, 215202.

(46). Liu SP; Artois J; Schmid D; Wieser M; Bornemann B; Weisbrod S; Marx A; Scheer E; Erbe A Electronic Transport through Short DsDNA Measured with Mechanically Controlled Break Junctions: New Thiol–Gold Binding Protocol Improves Conductance. Phys. status solidi 2013, 250, 2342–2348.

(47). Bruot C; Xiang L; Palma JL; Tao N Effect of Mechanical Stretching on DNA Conductance. ACS Nano 2015, 9, 88–94. [PubMed: 25530305]

(48). Liu S-P; Weisbrod SH; Tang Z; Marx A; Scheer E; Erbe A Direct Measurement of Electrical Transport Through G-Quadruplex DNA with Mechanically Controllable Break Junction Electrodes. Angew. Chemie Int. Ed 2010, 49, 3313–3316.

(49). Dulic D; Tuukkanen S; Chung CL; Isambert A; Lavie P; Filoramo A Direct Conductance Measurements of Short Single DNA Molecules in Dry Conditions. Nanotechnology 2009, 20, 115502. [PubMed: 19420440]

(50). Berlin YA; Burin AL; Ratner MA Charge Hopping in DNA. J. Am. Chem. Soc 2001, 123, 260–268. [PubMed: 11456512]

(51). Boon EM; Barton JK Charge Transport in DNA. Curr. Opin. Struct. Biol 2002, 12, 320–329. [PubMed: 12127450]

(52). Sontz PA; Muren NB; Barton JK DNA Charge Transport for Sensing and Signaling. Acc. Chem. Res 2012, 45, 1792–1800. [PubMed: 22861008]

(53). Giese B Long-Distance Charge Transport in DNA: The Hopping Mechanism. Acc. Chem. Res 2000, 33, 631–636. [PubMed: 10995201]

(54). Jortner J; Bixon M; Langenbacher T; Michel-Beyerle ME Charge Transfer and Transport in DNA. Proc. Natl. Acad. Sci 1998, 95, 12759–12765. [PubMed: 9788986]

(55). Li X-Q; Yan Y Electrical Transport through Individual DNA Molecules. Appl. Phys. Lett 2001, 79, 2190–2192.

(56). Cohen H; Nogues C; Naaman R; Porath D Direct Measurement of Electrical Transport through Single DNA Molecules of Complex Sequence. Proc. Natl. Acad. Sci 2005, 102, 11589–11593. [PubMed: 16087871]

(57). Porath D; Bezryadin A; de Vries S; Dekker C Direct Measurement of Electrical Transport through DNA Molecules. Nature 2000, 403, 635–638. [PubMed: 10688194]

(58). Zhang F; Guan Y; Yang Y; Hunt A; Wang S; Chen H-Y; Tao N Optical Tracking of Nanometer-Scale Cellular Membrane Deformation Associated with Single Vesicle Release. ACS Sensors 2019, 4, 2205–2212. [PubMed: 31348853]

(59). Zhu H; Zhang F; Wang H; Lu Z; Chen HY; Li J; Tao N Optical Imaging of Charges with Atomically Thin Molybdenum Disulfide. ACS Nano 2019, 13, 2298–2306. [PubMed: 30636406]

(60). Jiang D; Jiang Y; Li Z; Liu T; Wo X; Fang Y; Tao N; Wang W; Chen H-Y Optical Imaging of Phase Transition and Li-Ion Diffusion Kinetics of Single LiCoO 2 Nanoparticles During Electrochemical Cycling. J. Am. Chem. Soc 2017, 139, 186–192. [PubMed: 27959535]

(61). Zhu H; Ma G; Wan Z; Wang H; Tao N Detection of Molecules and Charges with a Bright Field Optical Microscope. Anal. Chem 2020, 92, 5904–5909.

(62). Guan Y; Shan X; Wang S; Zhang P; Tao N Detection of Molecular Binding via Charge-Induced Mechanical Response of Optical Fibers. Chem. Sci 2014, 5, 4375–4381. [PubMed: 25408862]

(63). Zhu H; Zhang F; Wang H; Lu Z; Chen HY; Li J; Tao N Optical Imaging of Charges with Atomically Thin Molybdenum Disulfide. ACS Nano 2019, 13, 2298–2306. [PubMed: 30636406]

(64). Ma G; Guan Y; Wang S; Xu H; Tao N Study of Small-Molecule–Membrane Protein Binding Kinetics with Nanodisc and Charge-Sensitive Optical Detection. Anal. Chem 2016, 88, 2375–2379. [PubMed: 26752355]

(65). Yang Y; Shen G; Wang H; Li H; Zhang T; Tao N; Ding X; Yu H Interferometric Plasmonic Imaging and Detection of Single Exosomes. Proc. Natl. Acad. Sci. U. S. A 2018, 115, 10275–10280. [PubMed: 30249664]

(66). Yu J; Qin X; Xian X; Tao N Oxygen Sensing Based on the Yellowing of Newspaper. ACS Sensors 2018, 3, 160–166. [PubMed: 29277997]

(67). Shao D; Yang Y; Liu C; Tsow F; Yu H; Tao N Noncontact Monitoring Breathing Pattern, Exhalation Flow Rate and Pulse Transit Time. IEEE Trans. Biomed. Eng 2014, 61, 2760–2767. [PubMed: 25330153]

(68). Phillips M; Cataneo RN; Cummin ARC; Gagliardi AJ; Gleeson K; Greenberg J; Maxfield RA; Rom WN Detection of Lung Cancer With Volatile Markers in the Breatha. Chest 2003, 123, 2115–2123. [PubMed: 12796197]

(69). Yu H; Shan X; Wang S; Chen H; Tao N Plasmonic Imaging and Detection of Single DNA Molecules. ACS Nano 2014, 8, 3427–3433. [PubMed: 24593238]

(70). Forzani ES; Zhang H; Chen W; Tao N Detection of Heavy Metal Ions in Drinking Water Using a High-Resolution Differential Surface Plasmon Resonance Sensor. Environ. Sci. Technol 2005, 39, 1257–1262. [PubMed: 15787364]

(71). Wang S; Forzani ES; Tao N Detection of Heavy Metal Ions in Water by High-Resolution Surface Plasmon Resonance Spectroscopy Combined with Anodic Stripping Voltammetry. Anal. Chem 2007, 79, 4427–4432. [PubMed: 17503766]

(72). Tao NJ; Lindsay SM; Lees S Measuring the Microelastic Properties of Biological Material. Biophys. J 1992, 63, 1165–1169. [PubMed: 1420932]

(73). Tao NJ; Lindsay SM; Rupprecht A The Dynamics of the DNA Hydration Shell at Gigahertz Frequencies. Biopolymers 1987, 26, 171–188. [PubMed: 3828471]

(74). Tao NJ; Lindsay SM; Rupprecht A Structure of DNA Hydration Shells Studied by Raman Spectroscopy. Biopolymers 1989, 28, 1019–1030. [PubMed: 2742983]

(75). Tao NJ; Lindsay SM; Rupprecht A Dynamic Coupling between DNA and Its Primary Hydration Shell Studied by Brillouin Scattering. Biopolymers 1988, 27, 1655–1671. [PubMed: 3233323]

(76). Tao NJ; Lindsay SM; Rupprecht A Dynamics of DNA Hydration Shells at GHz Frequencies Studied by Brillouin Scattering. Biopolymers 1987, 26, 171–188. [PubMed: 3828471]

(77). Weidlich T; Lee SA; Lindsay SM; Powell JW; Tao NJ; Lewen G; Rupprecht A A Brillouin-Scattering Study of the Hydration of Li-DNA and Na-DNA Films. Biophys. J 1987, 51, A282.

(78). DeRose JA; Thundat T; Nagahara LA; Lindsay SM Gold Grown Epitaxially on Mica: Conditions for Large Area Flat Faces. Surf. Sci. Lett 1991, 256, A533.

(79). Tao NJ; Lindsay SM Observations of the 22×√3 Reconstruction of Au(111) under Aqueous Solutions Using Scanning Tunneling Microscopy. J. Appl. Phys 1991, 70, 5141–5143.

(80). Tao NJ; Lindsay SM Kinetics of a Potential Induced to 1 × 1 Transition of Au(111) Studied by *In Situ* Scanning Tunneling Microscopy. Surf. Sci 1992, 274, L546–L553.

(81). Tao NJ; Pan J; Li Y; Oden PI; DeRose JA; Lindsay SM Initial Stage of Underpotential Deposition of Pb on Reconstructed and Unreconstructed Au(111). Surf. Sci 1992, 271, L338–L344.

(82). Tao NJ; Lindsay SM *In Situ* Scanning Tunneling Microscopy Study of Iodine and Bromine Adsorption on Gold(111) under Potential Control. J. Phys. Chem 1992, 96, 5213–5217.

(83). Tao NJ; DeRose JA; Lindsay SM Self-Assembly of Molecular Superstructures Studied by *In Situ* Scanning Tunneling Microscopy: DNA Bases on Gold (111). J. Phys. Chem 1993, 97, 910–919.

(84). Li YQ; Tao NJ; Pan J; Garcia AA; Lindsay SM Direct Measurement of Interaction Forces between Colloidal Particles Using the Scanning Force Microscope. Langmuir 1993, 9, 637–641.

(85). Pan J; Tao N; Lindsay SM An Atomic Force Microscopy Study of Self-Assembled Octadecyl Mercaptan Monolayer Adsorbed on Gold(111) under Potential Control. Langmuir 1993, 9, 1556–1560.

(86). Lees S; Tao NJ; Lindsay SM Studies of Compact Hard Tissues and Collagen by Means of Brillouin Light Scattering. Connect. Tissue Res 1990, 24, 187–205. [PubMed: 2376122]

(87). Tao NJ Probing Potential-Tuned Resonant Tunneling through Redox Molecules with Scanning Tunneling Microscopy. Phys. Rev. Lett 1996, 76, 4066–4069. [PubMed: 10061183]

(88). Giz M; Duong B; Tao N *In Situ* STM Study of Self-Assembled Mercaptopropionic Acid Monolayers for Electrochemical Detection of Dopamine. J. Electroanal. Chem 1999, 465, 72–79.

(89). Jin Q; Rodriguez J; Li C; Darici Y; Tao N Self-Assembly of Aromatic Thiols on Au(111). Surf. Sci 1999, 425, 101–111.

(90). Ke Y; Milano S; Wang X; Tao N; Darici Y Structural Studies of Sulfur-Passivated GaAs (100) Surfaces with LEED and AFM. Surf. Sci 1998, 415, 29–36.

(91). Cunha F; Tao NJ Surface Charge Induced Order-Disorder Transition in an Organic Monolayer. Phys. Rev. Lett 1995, 75, 2376–2379. [PubMed: 10059288]

(92). Domínguez O; Echegoyen L; Cunha F; Tao N Self-Assembled Fullerene-Derivative Monolayers on a Gold Substrate Using Phenanthroline-Au Interactions. Langmuir 1998, 14, 821–824.

(93). Cunha F; Jin Q; Tao NJ; Li CZ Structural Phase Transition in Self-Assembled 1,10′ Phenanthroline Monolayer on Au(111). Surf. Sci 1997, 389, 19–28.

(94). Cunha F; Tao NJ; Wang XW; Jin Q; Duong B; D'Agnese J Potential-Induced Phase Transitions in 2,2'-Bipyridine and 4,4'-Bipyridine Monolayers on Au(111) Studied by *In Situ* Scanning Tunneling Microscopy and Atomic Force Microscopy. Langmuir 1996, 12, 6410–6418.

(95). Wang XW; Tao NJ; Cunha F STM Images of Guanine on Graphite Surface and the Role of Tip–Sample Interaction. J. Chem. Phys 1996, 105, 3747–3752.

(96). Tao NJ; Shi Z Kinetics of Oxidation of Guanine Monolayers at the Graphite-Water Interface Studied by AFM/STM. J. Phys. Chem 1994, 98, 7422–7426.

(97). Tao NJ; Li CZ; He HX Scanning Tunneling Microscopy Applications in Electrochemistry - beyond Imaging. J. Electroanal. Chem 2000, 492, 81–93.

(98). Bard AJ; Faulkner LR Electrochemical Methods Fundamentals and Applications 2nd Ed. John Wiley&Sons, New Jersey, USA 2001.

(99). Xiang L; Tao NJ Reactions Triggered Electrically. Nature 2016, 531, 38–39. [PubMed: 26935691]

(100). Aragonès AC; Haworth NL; Darwish N; Ciampi S; Bloomfield NJ; Wallace GG; Diez-Perez I; Coote ML Electrostatic Catalysis of a Diels–Alder Reaction. Nature 2016, 531, 88–91. [PubMed: 26935697]

(101). Wang C; Danovich D; Chen H; Shaik S Oriented External Electric Fields: Tweezers and Catalysts for Reactivity in Halogen-Bond Complexes. J. Am. Chem. Soc 2019, 141, 7122–7136. [PubMed: 30945542]

(102). Dziri L; Boussaad S; Tao N; Leblanc RM Acetylcholinesterase Complexation with Acetylthiocholine or Organophosphate at the Air/Aqueous Interface: AFM and UV-Vis Studies. Langmuir 1998, 14, 4853–4859.

(103). Boussaad S; Dziri L; Arechabaleta R; Tao NJ; Leblanc RM Electron-Transfer Properties of Cytochrome c Langmuir-Blodgett Films and Interactions of Cytochrome c with Lipids. Langmuir 1998, 14, 6215–6219.

(104). Boussaad S; Tao NJ Electron Transfer and Adsorption of Myoglobin on Self-Assembled Surfactant Films: An Electrochemical Tapping-Mode AFM Study. J. Am. Chem. Soc 1999, 121, 4510–4515.

(105). Boussaad S; Tao NJ; Arechabaleta R Structural and Electron Transfer Properties of Cytochrome c Adsorbed on Graphite Electrode Studied by In-Situ Tapping Mode AFM. Chem. Phys. Lett 1997, 280, 397–403.

(106). Shao L; Tao NJ; Leblanc RM Probing the Microelastic Properties of Nanobiological Particles with Tapping Mode Atomic Force Microscopy. Chem. Phys. Lett 1997.

(107). Landman U; Luedtke WD; Salisbury BE; Whetten RL Reversible Manipulations of Room Temperature Mechanical and Quantum Transport Properties in Nanowire Junctions. Phys. Rev. Lett 1996, 77, 1362–1365. [PubMed: 10063057]

(108). Krans JM; van Ruitenbeek JM; Fisun VV; Yanson IK; de Jongh LJ The Signature of Conductance Quantization in Metallic Point Contacts. Nature 1995, 375, 767–769.

(109). van Ruitenbeek JM; Alvarez A; Piñeyro I; Grahmann C; Joyez P; Devoret MH; Esteve D; Urbina C Adjustable Nanofabricated Atomic Size Contacts. Rev. Sci. Instrum 1996, 67, 108–111.

(110). Gai Z; He Y; Yu H; Yang WS Observation of Conductance Quantization of Ballistic Metallic Point Contacts at Room Temperature. Phys. Rev. B 1996, 53, 1042–1045.

(111). Muller CJ; van Ruitenbeek JM; Beenakker CWJ; de Bruyn Ouboter R Conductance and Supercurrent Discontinuities in Atomic Size Point Contacts. Phys. B Condens. Matter 1993, 189, 225–234.

(112). va. den Brom HE; Yanson AI; va. Ruitenbeek JMCharacterization of Individual Conductance Steps in Metallic Quantum Point Contacts. Phys. B Condens. Matter 1998, 252, 69–75.

(113). Zhou X-S; Wei Y-M; Liu L; Chen Z-B; Tang J; Mao B-W Extending the Capability of STM Break Junction for Conductance Measurement of Atomic-Size Nanowires: An Electrochemical Strategy. J. Am. Chem. Soc 2008, 130, 13228–13230. [PubMed: 18788809]

(114). Chen R; Wheeler PJ; Natelson D Excess Noise in STM-Style Break Junctions at Room Temperature. Phys. Rev. B 2012, 85, 235455.

(115). Li CZ; Tao NJ Quantum Transport in Metallic Nanowires Fabricated by Electrochemical Deposition/Dissolution. Appl. Phys. Lett 1998, 72, 894–896.

(116). Xu B; Tao NJ Measurement of Single-Molecule Resistance by Repeated Formation of Molecular Junctions. Science 2003, 301, 1221–1223. [PubMed: 12947193]

(117). He HX; Li XL; Tao NJ; Nagahara LA; Amlani I; Tsui R Discrete Conductance Switching in Conducting Polymer Wires. Phys. Rev. B 2003, 68, 045302.

(118). He J; Chen F; Lindsay S; Nuckolls C Length Dependence of Charge Transport in Oligoanilines. Appl. Phys. Lett 2007, 90, 072112.

(119). Zhang HQ; Boussaad S; Tao NJ High-Performance Differential Surface Plasmon Resonance Sensor Using Quadrant Cell Photodetector. Rev. Sci. Instrum 2003, 74, 150–153.

(120). Forzani ES; Foley K; Westerhoff P; Tao N Detection of Arsenic in Groundwater Using a Surface Plasmon Resonance Sensor. Sensors Actuators B Chem 2007, 123, 82–88.

(121). Forzani ES; Zhang H; Nagahara LA; Amlani I; Tsui R; Tao N A Conducting Polymer Nanojunction Sensor for Glucose Detection. Nano Lett 2004, 4, 2519–2519.

(122). Gooding J; Hibbert D; Yang W Electrochemical Metal Ion Sensors. Exploiting Amino Acids and Peptides as Recognition Elements. Sensors 2001, 1, 75–90.

(123). Aguilar AD; Forzani ES; Li X; Tao N; Nagahara LA; Amlani I; Tsui R Chemical Sensors Using Peptide-Functionalized Conducting Polymer Nanojunction Arrays. Appl. Phys. Lett 2005, 87, 193108.

(124). Aguilar AD; Forzani ES; Nagahara LA; Amlani I; Tsui R; Tao NJ Breath Ammonia Sensor Based on Conducting Polymer Nanojunctions. IEEE Sens. J 2008, 8, 269–273.

(125). Murray BJ; Walter EC; Penner RM Amine Vapor Sensing with Silver Mesowires. Nano Lett 2004, 4, 665–670.

(126). Walter EC; Favier F; Penner RM Palladium Mesowire Arrays for Fast Hydrogen Sensors and Hydrogen-Actuated Switches. Anal. Chem 2002, 74. [PubMed: 11795821]

(127). Favier F Hydrogen Sensors and Switches from Electrodeposited Palladium Mesowire Arrays. Science 2001, 293, 2227–2231. [PubMed: 11567132]

(128). Forzani ES; Li X; Zhang P; Tao N; Zhang R; Amlani I; Tsui R; Nagahara LA Tuning the Chemical Selectivity of SWNT-FETs for Detection of Heavy-Metal Ions. Small 2006, 2, 1283–1291. [PubMed: 17192975]

(129). Dastagir T; Forzani ES; Zhang R; Amlani I; Nagahara LA; Tsui R; Tao N Electrical Detection of Hepatitis C Virus RNA on Single Wall Carbon Nanotube-Field Effect Transistors. Analyst 2007, 132, 738. [PubMed: 17646871]

(130). Tao N; Forzani E Systems and Methods for Integrated Electrochemical and Electrical Detection US8465634, 2013.

(131). Tao N; Forzani E; Aguilar AD Systems and Methods for Integrated Detection US8545683, 2013.

(132). Tao N; Forzani E; Iglesias RA Integrated Optoelectrochemical Sensor for Nitrogen Oxides in Gaseous Samples US9581561, 2014.

(133). Forzani E; Tao N; Xian X; Tsow F Mouthpiece for Accurate Detection of Exhaled NO US9931055, 2018.

(134). Prabhakar A; Iglesias RA; Wang R; Tsow F; Forzani ES; Tao N Ultrasensitive Detection of Nitrogen Oxides over a Nanoporous Membrane. Anal. Chem 2010, 82, 9938–9940. [PubMed: 21053913]

(135). Díaz Aguilar A; Forzani ES; Leright M; Tsow F; Cagan A; Iglesias RA; Nagahara LA; Amlani I; Tsui R; Tao NJ A Hybrid Nanosensor for TNT Vapor Detection. Nano Lett 2010, 10, 380–384. [PubMed: 20041699]

(136). Forzani ES; Lu D; Leright MJ; Aguilar AD; Tsow F; Iglesias RA; Zhang Q; Lu J; Li J; Tao N A Hybrid Electrochemical- Colorimetric Sensing Platform for Detection of Explosives. J. Am. Chem. Soc 2009, 131, 1390–1391. [PubMed: 19173664]

(137). Boussaad S; Tao NJ Polymer Wire Chemical Sensor Using a Microfabricated Tuning Fork. Nano Lett 2003, 3, 1173–1176.

(138). Tao N; Boussaad S Chemical and Biological Sensing Using Tuning Forks US Patent 8215170, 2012.

(139). Iglesias RA; Tsow F; Wang R; Forzani ES; Tao N Hybrid Separation and Detection Device for Analysis of Benzene, Toluene, Ethylbenzene, and Xylenes in Complex Samples. Anal. Chem 2009, 81, 8930–8935. [PubMed: 19780581]

(140). Tsow F; Forzani ES; Tao NJ Frequency-Coded Chemical Sensors. Anal. Chem 2008, 80, 606–611. [PubMed: 18163596]

(141). Ren M; Forzani ES; Tao N Chemical Sensor Based on Microfabricated Wristwatch Tuning Forks. Anal. Chem 2005, 77, 2700–2707. [PubMed: 15859583]

(142). Feng H; Lu J; Li J; Tsow F; Forzani E; Tao N Hybrid Mechanoresponsive Polymer Wires Under Force Activation. Adv. Mater 2013, 25, 1729–1733. [PubMed: 23280548]

(143). Tsow F; Forzani E; Rai A; Wang R; Tsui R; Mastroianni S; Knobbe C; Gandolfi AJ; Tao NJ A Wearable and Wireless Sensor System for Real-Time Monitoring of Toxic Environmental Volatile Organic Compounds. IEEE Sens. J 2009, 9, 1734–1740.

(144). Chen C; Driggs Campbell K; Negi I; Iglesias RA; Owens P; Tao N; Tsow F; Forzani ES A New Sensor for the Assessment of Personal Exposure to Volatile Organic Compounds. Atmos. Environ 2012, 54, 679–687.

(145). Chen C; Tsow F; Campbell KD; Iglesias R; Forzani E; Tao N A Wireless Hybrid Chemical Sensor for Detection of Environmental Volatile Organic Compounds. IEEE Sens. J 2013, 13, 1748–1755. [PubMed: 24078793]

(146). Deng Y; Chen C; Xian X; Tsow F; Verma G; McConnell R; Fruin S; Tao N; Forzani E A Novel Wireless Wearable Volatile Organic Compound (VOC) Monitoring Device with Disposable Sensors. Sensors 2016, 16, 2060.

(147). Qin X; Xian X; Deng Y; Wang D; Tsow F; Forzani E; Tao N Micro Quartz Tuning Fork-Based PM 2.5 Sensor for Personal Exposure Monitoring. IEEE Sens. J 2019, 19, 2482–2489.

(148). Rakow NA; Suslick KS A Colorimetric Sensor Array for Odour Visualization. Nature 2000, 406, 710–713. [PubMed: 10963592]

(149). Zhao D; Xian X; Terrera M; Krishnan R; Miller D; Bridgeman D; Tao K; Zhang L; Tsow F; Forzani ES; et al. A Pocket-Sized Metabolic Analyzer for Assessment of Resting Energy Expenditure. Clin. Nutr 2014, 33, 341–347. [PubMed: 23827182]

(150). Tao N; Forzani E Metabolic Analyzer US Patent 10143401, 2018.

(151). Tsow F; Xian X; Forzani E; Tao N Portable Metabolic Analyzer System US Patent 10078074B2, 2018.

(152). Stump C; Jackemeyer D; Abidov Y; Herbst K; Tao N; Forzani E Study of the Effect of Mobile Indirect Calorimeter on Weight Management. Glob. J. Obes. Diabetes Metab. Syndr 2017, 4, 44–50.

(153). Xian X; Tsow F; Rai S; Anderson T; Prabhakar A; Terrera M; Ainsworth B; Jackemeyer D; Quach A; Tao N; et al. Personal Mobile Tracking of Resting and Excess Post-Exercise Oxygen Consumption with a Mobile Indirect Calorimeter. Gazz. Medica Ital. Arch. per le Sci. Mediche 2020, 178, 868–879.

(154). Lin C; Xian X; Qin X; Wang D; Tsow F; Forzani E; Tao N High Performance Colorimetric Carbon Monoxide Sensor for Continuous Personal Exposure Monitoring. ACS Sensors 2018, 3, 327–333. [PubMed: 29299924]

(155). Lin C; Zhu Y; Yu J; Qin X; Xian X; Tsow F; Forzani ES; Wang D; Tao N Gradient-Based Colorimetric Sensors for Continuous Gas Monitoring. Anal. Chem 2018, 90, 5375–5380. [PubMed: 29607646]

(156). Qin X; Wang R; Tsow F; Forzani E; Xian X; Tao N A Colorimetric Chemical Sensing Platform for Real-Time Monitoring of Indoor Formaldehyde. IEEE Sens. J 2015, 15, 1545–1551.

(157). Wang R; Prabhakar A; Iglesias RA; Xian X; Shan X; Tsow F; Forzani ES; Tao N A Microfluidic-Colorimetric Sensor for Continuous Monitoring of Reactive Environmental Chemicals. IEEE Sens. J 2012, 12, 1529–1535.

(158). Mallires KR; Wang D; Tipparaju VV; Tao N Developing a Low-Cost Wearable Personal Exposure Monitor for Studying Respiratory Diseases Using Metal–Oxide Sensors. IEEE Sens. J 2019, 19, 8252–8261.

(159). Tipparaju VV; Xian X; Bridgeman D; Wang D; Tsow F; Forzani E; Tao N Reliable Breathing Tracking With Wearable Mask Device. IEEE Sens. J 2020, 20, 5510–5518.

(160). Shao D; Liu C; Tsow F; Yang Y; Du Z; Iriya R; Yu H; Tao N Noncontact Monitoring of Blood Oxygen Saturation Using Camera and Dual-Wavelength Imaging System. IEEE Trans. Biomed. Eng 2016, 63, 1091–1098. [PubMed: 26415199]

(161). Tao NJ Electron Transport in Molecular Junctions. Nat. Nanotechnol 2006, 1, 173–181. [PubMed: 18654182]

(162). Enoki T; Kiguchi M Challenges for Single Molecule Electronic Devices with Nanographene and Organic Molecules. Do Single Molecules Offer Potential as Elements of Electronic Devices in the next Generation? Phys. Scr 2018, 93, 053001.

(163). Aviram A; Ratner MA Molecular Rectifiers. Chem. Phys. Lett 1974, 29, 277–283.

(164). Reddy P; Jang S-Y; Segalman RA; Majumdar A Thermoelectricity in Molecular Junctions. Science 2007, 315, 1568–1571. [PubMed: 17303718]

(165). Venkataraman L; Klare JE; Nuckolls C; Hybertsen MS; Steigerwald ML Dependence of Single-Molecule Junction Conductance on Molecular Conformation. Nature 2006, 442, 904–907. [PubMed: 16929295]

(166). Woitellier S; Launay JP; Joachim C The Possibility of Molecular Switching: Theoretical Study of [(NH3)5Ru-4,4′-Bipy-Ru(NH3)5]5+. Chem. Phys 1989, 131, 481–488.

(167). Lindsay SM; Ratner MA Molecular Transport Junctions: Clearing Mists. Adv. Mater 2007, 19, 23–31.

(168). Molecular Electronics under the Microscope. Nat. Chem 2015, 7, 181–181. [PubMed: 25698315]

(169). Chen F; Li X; Hihath J; Huang Z; Tao N Effect of Anchoring Groups on Single-Molecule Conductance: Comparative Study of Thiol-, Amine-, and Carboxylic-Acid-Terminated Molecules. J. Am. Chem. Soc 2006, 128, 15874–15881. [PubMed: 17147400]

(170). Li X; He J; Hihath J; Xu B; Lindsay SM; Tao N Conductance of Single Alkanedithiols: Conduction Mechanism and Effect of Molecule-Electrode Contacts. J. Am. Chem. Soc 2006, 128, 2135–2141. [PubMed: 16464116]

(171). Haiss W; Nichols RJ; van Zalinge H; Higgins SJ; Bethell D; Schiffrin DJ Measurement of Single Molecule Conductivity Using the Spontaneous Formation of Molecular Wires. Phys. Chem. Chem. Phys 2004, 6, 4330.

(172). Haiss W; Wang C; Grace I; Batsanov AS; Schiffrin DJ; Higgins SJ; Bryce MR; Lambert CJ; Nichols RJ Precision Control of Single-Molecule Electrical Junctions. Nat. Mater 2006, 5, 995–1002. [PubMed: 17128259]

(173). Xia JL; Diez-Perez I; Tao NJ Electron Transport in Single Molecules Measured by a Distance-Modulation Assisted Break Junction Method. Nano Lett 2008, 8, 1960–1964. [PubMed: 18543978]

(174). Diez-Perez I; Hihath J; Hines T; Wang Z-S; Zhou G; Müllen K; Tao N Controlling Single-Molecule Conductance through Lateral Coupling of π Orbitals. Nat. Nanotechnol 2011, 6, 226–231. [PubMed: 21336268]

(175). Jiang P; Morales GM; You W; Yu L Synthesis of Diode Molecules and Their Sequential Assembly to Control Electron Transport. Angew. Chemie Int. Ed 2004, 43, 4471–4475.

(176). Elbing M; Ochs R; Koentopp M; Fischer M; von Hanisch C; Weigend F; Evers F; Weber HB; Mayor M A Single-Molecule Diode. Proc. Natl. Acad. Sci 2005, 102, 8815–8820. [PubMed: 15956208]

(177). Díez-Pérez I; Hihath J; Lee Y; Yu L; Adamska L; Kozhushner MA; Oleynik II; Tao N Rectification and Stability of a Single Molecular Diode with Controlled Orientation. Nat. Chem 2009, 1, 635–641. [PubMed: 21378955]

(178). Bruot C; Hihath J; Tao N Mechanically Controlled Molecular Orbital Alignment in Single Molecule Junctions. Nat. Nanotechnol 2012, 7, 35–40.

(179). Todorov TN; Hoekstra J; Sutton AP Current-Induced Forces in Atomic-Scale Conductors. Philos. Mag. B 2000, 80, 421–455.

(180). Todorov TN Local Heating in Ballistic Atomic-Scale Contacts. Philos. Mag. B 1998, 77, 965–973.

(181). Huang Z; Chen F; D'agosta R; Bennett PA; Di Ventra M; Tao N Local Ionic and Electron Heating in Single-Molecule Junctions. Nat. Nanotechnol 2007, 2, 698–703. [PubMed: 18654408]

(182). Huang; Xu; Chen; Di Ventra M; Tao. Measurement of Current-Induced Local Heating in a Single Molecule Junction. Nano Lett 2006, 6, 1240–1244. [PubMed: 16771587]

(183). D'Agosta R; Di. Ventra M Hydrodynamic Approach to Transport and Turbulence in Nanoscale Conductors. J. Phys. Condens. Matter 2006, 18, 11059–11065.

(184). Xu; Xiao; Yang X; Zang L; Tao. Large Gate Modulation in the Current of a Room Temperature Single Molecule Transistor. J. Am. Chem. Soc 2005, 127, 2386–2387. [PubMed: 15724981]

(185). Xu BQ; Li XL; Xiao XY; Sakaguchi H; Tao NJ Electromechanical and Conductance Switching Properties of Single Oligothiophene Molecules. Nano Lett 2005, 5, 1491–1495. [PubMed: 16178263]

(186). Xiao X; Nagahara LA; Rawlett AM; Tao N Electrochemical Gate-Controlled Conductance of Single Oligo(Phenylene Ethynylene)S. J. Am. Chem. Soc 2005, 127, 9235–9240. [PubMed: 15969602]

(187). Xiao X; Brune D; He J; Lindsay S; Gorman CB; Tao N Redox-Gated Electron Transport in Electrically Wired Ferrocene Molecules. Chem. Phys 2006, 326, 138–143.

(188). Chen F; Qing Q; Xia J; Li J; Tao N Electrochemical Gate-Controlled Charge Transport in Graphene in Ionic Liquid and Aqueous Solution. J. Am. Chem. Soc 2009, 131, 9908–9909. [PubMed: 19572712]

(189). Diez-Perez I; Li Z; Hihath J; Li J; Zhang C; Yang X; Zang L; Dai Y; Feng X; Muellen K; et al. Gate-Controlled Electron Transport in Coronenes as a Bottom-up Approach towards Graphene Transistors. Nat. Commun 2010, 1, 31. [PubMed: 20975686]

(190). Darwish N; Díez-Pérez I; Guo S; Tao N; Gooding JJ; Paddon-Row MN Single Molecular Switches: Electrochemical Gating of a Single Anthraquinone-Based Norbornylogous Bridge Molecule. J. Phys. Chem. C 2012, 116, 21093–21097.

(191). Díez-Pérez I; Li Z; Guo S; Madden C; Huang H; Che Y; Yang X; Zang L; Tao N Ambipolar Transport in an Electrochemically Gated Single-Molecule Field-Effect Transistor. ACS Nano 2012, 6, 7044–7052. [PubMed: 22789617]

(192). Li; Hihath J; Chen F; Masuda T; Zang L; Tao. Thermally Activated Electron Transport in Single Redox Molecules. J. Am. Chem. Soc 2007, 129, 11535–11542. [PubMed: 17718563]

(193). Hihath J; Arroyo CR; Rubio-Bollinger G; Tao N; Agraït N Study of Electron-Phonon Interactions in a Single Molecule Covalently Connected to Two Electrodes. Nano Lett 2008, 8, 1673–1678. [PubMed: 18457456]

(194). Hihath J; Bruot C; Tao N Electron-Phonon Interactions in Single Octanedithiol Molecular Junctions. ACS Nano 2010, 4, 3823–3830. [PubMed: 20553018]

(195). Hines T; Diez-Perez I; Hihath J; Liu H; Wang Z-S; Zhao J; Zhou G; Müllen K; Tao N Transition from Tunneling to Hopping in Single Molecular Junctions by Measuring Length and Temperature Dependence. J. Am. Chem. Soc 2010, 132, 11658–11664. [PubMed: 20669945]

(196). Hihath J; Bruot C; Nakamura H; Asai Y; Díez-Pérez I; Lee Y; Yu L; Tao N Inelastic Transport and Low-Bias Rectification in a Single-Molecule Diode. ACS Nano 2011, 5, 8331–8339. [PubMed: 21932824]

(197). Guo S; Zhou G; Tao N Single Molecule Conductance, Thermopower, and Transition Voltage. Nano Lett 2013, 13, 4326–4332. [PubMed: 23895464]

(198). Xiang L; Hines T; Palma JL; Lu X; Mujica V; Ratner MA; Zhou G; Tao N Non-Exponential Length Dependence of Conductance in Iodide-Terminated Oligothiophene Single-Molecule Tunneling Junctions. J. Am. Chem. Soc 2016, 138, 679–687. [PubMed: 26694660]

(199). Aragones AC; Medina E; Ferrer-Huerta M; Gimeno N; Teixido M; Palma JL; Tao N; Ugalde JM; Giralt E; Diez-Perez I Measuring the Spin-Polarization Power of a Single Chiral Molecule. Small 2017, 13.

(200). Seeman NC; Sleiman HF DNA Nanotechnology. Nat. Rev. Mater 2018, 3, 17068.

(201). Garibotti AV; Knudsen SM; Ellington AD; Seeman NC Functional DNAzymes Organized into Two-Dimensional Arrays. Nano Lett 2006, 6, 1505–1507. [PubMed: 16834439]

(202). Torring T; Voigt NV; Nangreave J; Yan H; Gothelf KV DNA Origami: A Quantum Leap for Self-Assembly of Complex Structures. Chem. Soc. Rev 2011, 40, 5636–5646. [PubMed: 21594298]

(203). Jiang Q; Song C; Nangreave J; Liu X; Lin L; Qiu D; Wang Z-G; Zou G; Liang X; Yan H; et al. DNA Origami as a Carrier for Circumvention of Drug Resistance. J. Am. Chem. Soc 2012, 134, 13396–13403. [PubMed: 22803823]

(204). Liu N; Liedl T DNA-Assembled Advanced Plasmonic Architectures. Chem. Rev 2018, 118, 3032–3053. [PubMed: 29384370]

(205). Deng Z; Mao C Molecular Lithography with DNA Nanostructures. Angew. Chemie Int. Ed 2004, 43, 4068–4070.

(206). Xu B; Tao NJ Measurement of Single-Molecule Resistance by Repeated Formation of Molecular Junctions. Science 2003, 301, 1221–1223. [PubMed: 12947193]

(207). Tao NJ; DeRose JA; Lindsay SM Self-Assembly of Molecjular Superstructures Studied by In-Situ Scanning Tunneling Microscopy - DNA Bases on Au(111). J. Phys. Chem 1993, 97, 910–919.

(208). Braun E; Eichen Y; Sivan U; Ben-Yoseph G DNA-Templated Assembly and Electrode Attachment of a Conducting Silver Wire. Nature 1998, 391, 775–778. [PubMed: 9486645]

(209). Storm AJ; Noort J van de Vries S; Dekker C Insulating Behavior for DNA Molecules between Nanoelectrodes at the 100 Nm Length Scale. Appl. Phys. Lett 2001, 79, 3881–3883.

(210). Porath D; Bezryadin A; de Vries S; Dekker C Direct Measurement of Electrical Transport through DNA Molecules. Nature 2000, 403, 635–638. [PubMed: 10688194]

(211). Fink HW; Schonenberger C Electrical Conduction through DNA Molecules. Nature 1999, 398, 407–410. [PubMed: 10201370]

(212). Kasumov AY; Kociak M; Gueron S; Reulet B; Volkov VT; Klinov DV; Bouchiat H Proximity-Induced Superconductivity in DNA. Science 2001, 291, 280–282. [PubMed: 11209072]

(213). O'Neill MA; Barton JK DNA-Mediated Charge Transport Chemistry and Biology. Long-Range Charg. Transf. DNA I 2004, 236, 67–115.

(214). Lewis F; Wu T; Zhang Y; Letsinger R; Greenfield S; Wasielewski M Distance-Dependent Electron Transfer in DNA Hairpins. Science 1997, 277, 673–676. [PubMed: 9235887]

(215). Hall DB; Holmlin RE; Barton JK Oxidative DNA Damage through Long-Range Electron Transfer. Nature 1996, 382, 731–735. [PubMed: 8751447]

(216). Bixon M; Jortner J Charge Transport in DNA *via* Thermally Induced Hopping. J. Am. Chem. Soc 2001, 123, 12556–12567. [PubMed: 11741420]

(217). Tao NJ Probing Potential-Tuned Resonant Tunneling through Redox Molecules with Scanning Tunneling Microscopy. Phys. Rev. Lett 1996, 76, 4066–4069. [PubMed: 10061183]

(218). Xu BQ; Zhang PM; Li XL; Tao NJ Direct Conductance Measurement of Single DNA Molecules in Aqueous Solution. Nano Lett 2004, 4, 1105–1108.

(219). Lewis FD; Liu X; Liu J; Miller SE; Hayes RT; Wasielewski MR Direct Measurement of Hole Transport Dynamics in DNA. Nature 2000, 406, 51–53. [PubMed: 10894536]

(220). Bixon M; Giese B; Wessely S; Langenbacher T; Michel-Beyerle ME; Jortner J Long-Range Charge Hopping in DNA. Proc. Natl. Acad. Sci. U. S. A 1999, 96, 11713–11716. [PubMed: 10518515]

(221). van Zalinge H; Schiffrin DJ; Bates AD; Starikov EB; Wenzel W; Nichols RJ Variable-Temperature Measurements of the Single-Molecule Conductance of Double-Stranded DNA. Angew. Chemie, Int. Ed. English 2006, 45, 5499–5502.

(222). Dulic D; Tuukkanen S; Chung CL; Isambert A; Lavie P; Filoramo A Direct Conductance Measurements of Short Single DNA Molecules in Dry Conditions. Nanotechnology 2009, 20, 115502. [PubMed: 19420440]

(223). Liu SP; Artois J; Schmid D; Wieser M; Bornemann B; Weisbrod S; Marx A; Scheer E; Erbe A Electronic Transport through Short DsDNA Measured with Mechanically Controlled Break Junctions: New Thiol–Gold Binding Protocol Improves Conductance. Phys. status solidi 2013, 250, 2342–2348.

(224). Ha DH; Nham H; Yoo K-H; So HL; Hae-Yeon; Kawai T Humidity Effects on the Conductance of the Assembly of DNA Molecules. Chem. Phys. Lett 2002, 355, 405–409.

(225). Cai L; Tabata H; Kawai T Self-Assembled DNA Networks and Their Electrical Conductivity. Appl. Phys. Lett 2000, 77, 3105–3106.

(226). Porath D; Cuniberti G; Di Felice R Charge Transport in DNA-Based Devices. Long-Range Charg. Transf. DNA II 2004, 237, 183–227.

(227). van Zalinge H; Schiffrin DJ; Bates AD; Haiss W; Ulstrup J; Nichols RJ Single-Molecule Conductance Measurements of Single- and Double-Stranded DNA Oligonucleoticles. ChemPhysChem 2006, 7, 94–98. [PubMed: 16345118]

(228). He J; Lin L; Liu H; Zhang P; Lee M; Sankey OF; Lindsay SM A Hydrogen-Bonded Electron-Tunneling Circuit Reads the Base Composition of Unmodified DNA. Nanotechnology 2009, 20, 075102. [PubMed: 19417406]

(229). Artés JM; Li Y; Qi J; Anantram MP; Hihath J Conformational Gating of DNA Conductance. Nat. Commun 2015, 6, 8870. [PubMed: 26648400]

(230). Li Y; Artés JM; Qi J; Morelan IA; Feldstein P; Anantram MP; Hihath J Comparing Charge Transport in Oligonucleotides: RNA:DNA Hybrids and DNA Duplexes. J. Phys. Chem. Lett 2016, 7, 1888–1894. [PubMed: 27145167]

(231). Livshits GI; Stern A; Rotem D; Borovok N; Eidelshtein G; Migliore A; Penzo E; Wind SJ; Di Felice R; Skourtis SS; et al. Long-Range Charge Transport in Single G-Quadruplex DNA Molecules. Nat. Nanotechnol 2014, 9, 1040–1046. [PubMed: 25344689]

(232). Sha R; Xiang L; Liu C; Balaeff A; Zhang Y; Zhang P; Li Y; Beratan DN; Tao N; Seeman NC Charge Splitters and Charge Transport Junctions Based on Guanine Quadruplexes. Nat. Nanotechnol 2018, 13, 316–321. [PubMed: 29483600]

(233). Liu S-P; Weisbrod SH; Tang Z; Marx A; Scheer E; Erbe A Direct Measurement of Electrical Transport Through G-Quadruplex DNA with Mechanically Controllable Break Junction Electrodes. Angew. Chemie Int. Ed 2010, 49, 3313–3316.

(234). Bruot C; Palma JL; Xiang L; Mujica V; Ratner MA; Tao N Piezoresistivity in Single DNA Molecules. Nat. Commun 2015, 6, 8032. [PubMed: 26337293]

(235). Bruot C; Xiang L; Palma JL; Tao N Effect of Mechanical Stretching on DNA Conductance. ACS Nano 2015, 9, 88–94. [PubMed: 25530305]

(236). Bruot C; Xiang L; Palma JL; Li Y; Tao N Tuning the Electromechanical Properties of Single DNA Molecular Junctions. J. Am. Chem. Soc 2015, 137, 13933–13937. [PubMed: 26480049]

(237). Li Y; Xiang L; Palma JL; Asai Y; Tao N Thermoelectric Effect and Its Dependence on Molecular Length and Sequence in Single DNA Molecules. Nat. Commun 2016, 7, 11294. [PubMed: 27079152]

(238). Rascon-Ramos H; Artes JM; Li Y; Hihath J Binding Configurations and Intramolecular Strain in Single-Molecule Devices. Nat. Mater 2015, 14, 517–522. [PubMed: 25686263]

(239). Xiang L; Palma JL; Bruot C; Mujica V; Ratner MA; Tao N Intermediate Tunnelling–Hopping Regime in DNA Charge Transport. Nat. Chem 2015, 7, 221–226. [PubMed: 25698331]

(240). Liu C; Xiang L; Zhang Y; Zhang P; Beratan DN; Li Y; Tao N Engineering Nanometre-Scale Coherence in Soft Matter. Nat. Chem 2016, 8, 941–945. [PubMed: 27657870]

(241). Li Y; Artés JM; Hihath J Long-Range Charge Transport in Adenine-Stacked RNA:DNA Hybrids. Small 2016, 12, 432–437. [PubMed: 26596516]

(242). Renaud N; Harris MA; Singh APN; Berlin YA; Ratner MA; Wasielewski MR; Lewis FD; Grozema FC Deep-Hole Transfer Leads to Ultrafast Charge Migration in DNA Hairpins. Nat. Chem 2016, 8, 1015–1021. [PubMed: 27768107]

(243). Michaeli K; Beratan DN; Waldeck DH; Naaman R Voltage-Induced Long-Range Coherent Electron Transfer through Organic Molecules. Proc. Natl. Acad. Sci 2019, 116, 5931–5936. [PubMed: 30846547]

(244). Hihath J; Xu B; Zhang P; Tao N Study of Single-Nucleotide Polymorphisms by Means of Electrical Conductance Measurements. Proc. Natl. Acad. Sci. U. S. A 2005, 102, 16979–16983. [PubMed: 16284253]

(245). Hihath J; Guo S; Zhang P; Tao N Effects of Cytosine Methylation on DNA Charge Transport. J. Phys. Condens. Matter 2012, 24, 164204. [PubMed: 22466008]

(246). Wang H; Muren NB; Ordinario D; Gorodetsky AA; Barton JK; Nuckolls C Transducing Methyltransferase Activity into Electrical Signals in a Carbon Nanotube-DNA Device. Chem. Sci 2012, 3, 62–65. [PubMed: 22822424]

(247). Li Y; Artés JM; Demir B; Gokce S; Mohammad HM; Alangari M; Anantram MP; Oren EE; Hihath J Detection and Identification of Genetic Material via Single-Molecule Conductance. Nat. Nanotechnol 2018, 13, 1167–1173. [PubMed: 30397286]

(248). Guo X; Gorodetsky AA; Hone J; Barton JK; Nuckolls C Conductivity of a Single DNA Duplex Bridging a Carbon Nanotube Gap. Nat Nano 2008, 3, 163–167.

(249). Xiang L; Palma JL; Li Y; Mujica V; Ratner MA; Tao N Gate-Controlled Conductance Switching in DNA. Nat. Commun 2017, 8, 14471. [PubMed: 28218275]

(250). Harashima T; Kojima C; Fujii S; Kiguchi M; Nishino T Single-Molecule Conductance of DNA Gated and Ungated by DNA-Binding Molecules. Chem. Commun 2017, 53, 10378–10381.

(251). Liu S; Clever GH; Takezawa Y; Kaneko M; Tanaka K; Guo X; Shionoya M Direct Conductance Measurement of Individual Metallo-DNA Duplexes within Single-Molecule Break Junctions. Angew. Chemie Int. Ed 2011, 50, 8886–8890.

(252). Eidelshtein G; Fardian-Melamed N; Gutkin V; Basmanov D; Klinov D; Rotem D; Levi-Kalisman Y; Porath D; Kotlyar A Synthesis and Properties of Novel Silver-Containing DNA Molecules. Adv. Mater 2016, 28, 4839–4844. [PubMed: 27116695]

(253). Guo C; Wang K; Zerah-Harush E; Hamill J; Wang B; Dubi Y; Xu B Molecular Rectifier Composed of DNA with High Rectification Ratio Enabled by Intercalation. Nat. Chem 2016, 8, 484–490. [PubMed: 27102683]

(254). Liu R; Ke S-H; Yang W; Baranger HU Organometallic Molecular Rectification. J. Chem. Phys 2006, 124, 024718. [PubMed: 16422637]

(255). Church GM; Gao Y; Kosuri S Next-Generation Digital Information Storage in DNA. Science 2012, 337, 1628–1628. [PubMed: 22903519]

(256). Zhao M; Chen Y; Wang K; Zhang Z; Streit JK; Fagan JA; Tang J; Zheng M; Yang C; Zhu Z DNA-Directed Nanofabrication of High-Performance Carbon Nanotube Field-Effect Transistors. Science 2020, 368, 878–881.

(257). Sanchez C Metal-like Conductivity in Microbial Nanowires. Nat. Rev. Microbiol 2011, 9, 700–700.

(258). Grubb DT Optical Microscopy In Polymer Science: A Comprehensive Reference; Elsevier, 2012; Vol. 10, pp 465–478.

(259). Schmolze DB; Standley C; Fogarty KE; Fischer AH Advances in Microscopy Techniques. Arch. Pathol. Lab. Med 2011, 135, 255–263. [PubMed: 21284447]

(260). Betzig E Single Molecules, Cells, and Super-Resolution Optics (Nobel Lecture). Angew. Chemie Int Ed. 2015, 54, 8034–8053.

(261). Wang W; Foley K; Shan X; Wang S; Eaton S; Nagaraj VJ; Wiktor P; Patel U; Tao N Single Cells and Intracellular Processes Studied by a Plasmonic-Based Electrochemical Impedance Microscopy. Nat. Chem 2011, 3, 249–255. [PubMed: 21336333]

(262). Yuan L; Tao N; Wang W Plasmonic Imaging of Electrochemical Impedance. Annu Rev Anal Chem (Palo Alto Calif) 2017, 10, 183–200. [PubMed: 28301751]

(263). Huang B; Yu F; Zare RN Surface Plasmon Resonance Imaging Using a High Numerical Aperture Microscope Objective. Anal. Chem 2007, 79, 2979–2983. [PubMed: 17309232]

(264). Zhou XL; Yang Y; Wang S; Liu XW Surface Plasmon Resonance Microscopy: From Single-Molecule Sensing to Single-Cell Imaging. Angew. Chemie 2020, 59, 1776–1785.

(265). Lindholm-Sethson B; Nystrom J; Malmsten M; Ringstad L; Nelson A; Geladi P Electrochemical Impedance Spectroscopy in Label-Free Biosensor Applications: Multivariate Data Analysis for an Objective Interpretation. Anal Bioanal Chem 2010, 398, 2341–2349. [PubMed: 20676616]

(266). Shan X; Díez-Pérez I; Wang L; Wiktor P; Gu Y; Zhang L; Wang W; Lu J; Wang S; Gong Q; et al. Imaging the Electrocatalytic Activity of Single Nanoparticles. Nat. Nanotechnol 2012, 7, 668–672. [PubMed: 22922540]

(267). Wang Y; Shan X; Wang H; Wang S; Tao N Plasmonic Imaging of Surface Electrochemical Reactions of Single Gold Nanowires. J. Am. Chem. Soc 2017, 139, 1376–1379. [PubMed: 28088852]

(268). Chen J; Zhou K; Wang Y; Gao J; Yuan T; Pang J; Tang S; Chen HY; Wang W Measuring the Activation Energy Barrier for the Nucleation of Single Nanosized Vapor Bubbles. Proc. Natl. Acad. Sci. U. S. A 2019, 116, 12678–12683. [PubMed: 31189597]

(269). Jiang Y; Su H; Wei W; Wang Y; Chen HY; Wang W Tracking the Rotation of Single CdS Nanorods during Photocatalysis with Surface Plasmon Resonance Microscopy. Proc. Natl. Acad. Sci. U. S. A 2019, 116, 6630–6634. [PubMed: 30872472]

(270). Fang Y; Li Z; Jiang Y; Wang X; Chen HY; Tao N; Wang W Intermittent Photocatalytic Activity of Single CdS Nanoparticles. Proc. Natl. Acad. Sci. U. S. A 2017, 114, 10566–10571. [PubMed: 28923941]

(271). Chen Z; Shan X; Guan Y; Wang S; Zhu J-J; Tao N Imaging Local Heating and Thermal Diffusion of Nanomaterials with Plasmonic Thermal Microscopy. ACS Nano 2015, 9, 11574–11581. [PubMed: 26435320]

(272). Yang Y; Shen G; Wang H; Li H; Zhang T; Tao N; Ding X; Yu H Interferometric Plasmonic Imaging and Detection of Single Exosomes. Proc. Natl. Acad. Sci. U. S. A 2018, 115, 10275–10280. [PubMed: 30249664]

(273). Yang Y; Yu H; Shan X; Wang W; Liu X; Wang S; Tao N Label-Free Tracking of Single Organelle Transportation in Cells with Nanometer Precision Using a Plasmonic Imaging Technique. Small 2015, 11, 2878–2884. [PubMed: 25703098]

(274). Jing W; Wang Y; Yang Y; Wang Y; Ma G; Wang S; Tao N Time-Resolved Digital Immunoassay for Rapid and Sensitive Quantitation of Procalcitonin with Plasmonic Imaging. ACS Nano 2019, 13, 8609–8617. [PubMed: 31276361]

(275). Shan X; Fang Y; Wang S; Guan Y; Chen H-Y; Tao N Detection of Charges and Molecules with Self-Assembled Nano-Oscillators. Nano Lett 2014, 14, 4151–4157. [PubMed: 24942903]

(276). Ma G; Shan X; Wang S; Tao N Quantifying Ligand–Protein Binding Kinetics with Self-Assembled Nano-Oscillators. Anal. Chem 2019, 91, 14149–14156. [PubMed: 31593433]

(277). Fang Y; Chen S; Wang W; Shan X; Tao N Real-Time Monitoring of Phosphorylation Kinetics with Self-Assembled Nano-oscillators. Angew. Chemie Int. Ed 2015, 54, 2538–2542.

(278). Wang W; Yang Y; Wang S; Nagaraj VJ; Liu Q; Wu J; Tao N Label-Free Measuring and Mapping of Binding Kinetics of Membrane Proteins in Single Living Cells. Nat. Chem 2012, 4, 846–853. [PubMed: 23000999]

(279). Wang W; Yin L; Gonzalez-Malerva L; Wang S; Yu X; Eaton S; Zhang S; Chen H-Y; LaBaer J; Tao N *In Situ* Drug-Receptor Binding Kinetics in Single Cells: A Quantitative Label-Free Study of Anti-Tumor Drug Resistance. Sci. Rep 2015, 4, 6609.

(280). Lu J; Li J Label-Free Imaging of Dynamic and Transient Calcium Signaling in Single Cells. Angew. Chemie 2015, 54, 13576–13580.

(281). Lu J; Yang Y; Wang W; Li J; Tao N; Wang S Label-Free Imaging of Histamine Mediated G Protein-Coupled Receptors Activation in Live Cells. Anal. Chem 2016, 88, 11498–11503. [PubMed: 27802015]

(282). Syal K; Wang W; Shan X; Wang S; Chen HY; Tao N Plasmonic Imaging of Protein Interactions with Single Bacterial Cells. Biosens. Bioelectron 2015, 63, 131–137. [PubMed: 25064821]

(283). Zhang F; Wang S; Yin L; Yang Y; Guan Y; Wang W; Xu H; Tao N Quantification of Epidermal Growth Factor Receptor Expression Level and Binding Kinetics on Cell Surfaces by Surface Plasmon Resonance Imaging. Anal. Chem 2015, 87, 9960–9965. [PubMed: 26368334]

(284). Syal K; Iriya R; Yang Y; Yu H; Wang S; Haydel SE; Chen H-Y; Tao N Antimicrobial Susceptibility Test with Plasmonic Imaging and Tracking of Single Bacterial Motions on Nanometer Scale. ACS Nano 2016, 10, 845–852. [PubMed: 26637243]

(285). Liu X-W; Yang Y; Wang W; Wang S; Gao M; Wu J; Tao N Plasmonic-Based Electrochemical Impedance Imaging of Electrical Activities in Single Cells. Angew. Chemie Int. Ed 2017, 56, 8855–8859.

(286). Guan Y; Shan X; Zhang F; Wang S; Chen H-Y; Tao N Kinetics of Small Molecule Interactions with Membrane Proteins in Single Cells Measured with Mechanical Amplification. Sci. Adv 2015, 1, e1500633. [PubMed: 26601298]

(287). Zhang F; Jing W; Hunt A; Yu H; Yang Y; Wang S; Chen H-Y; Tao N Label-Free Quantification of Small-Molecule Binding to Membrane Proteins on Single Cells by Tracking Nanometer-Scale Cellular Membrane Deformation. ACS Nano 2018, 12, 2056–2064. [PubMed: 29397682]

(288). Swinney DC The Role of Binding Kinetics in Therapeutically Useful Drug Action. Curr. Opin. Drug Discov. Devel 2009, 12, 31–39.

(289). Cho W; Stahelin RV Membrane-Protein Interactions in Cell Signaling and Membrane Trafficking. Annu Rev Biophys Biomol Struct 2005, 34, 119–151. [PubMed: 15869386]

(290). Yu H; Yang Y; Yang Y; Zhang F; Wang S; Tao N Tracking Fast Cellular Membrane Dynamics with Sub-Nm Accuracy in the Normal Direction. Nanoscale 2018, 10, 5133–5139. [PubMed: 29488990]

(291). Zhang F; Guan Y; Yang Y; Hunt A; Wang S; Chen H-Y; Tao N Optical Tracking of Nanometer-Scale Cellular Membrane Deformation Associated with Single Vesicle Release. ACS Sensors 2019, 4, 2205–2212. [PubMed: 31348853]

(292). Wang H; Shan X; Yu H; Wang Y; Schmickler W; Chen HY; Tao N Determining Electrochemical Surface Stress of Single Nanowires. Angew. Chemie 2017, 56, 2132–2135.

(293). Yang Y; Liu X-W; Wang H; Yu H; Guan Y; Wang S; Tao N Imaging Action Potential in Single Mammalian Neurons by Tracking the Accompanying Sub-Nanometer Mechanical Motion. ACS Nano 2018, 12, 4186–4193. [PubMed: 29570267]

(294). Kelly Spencer, Measure your breathing, lose weight?, BBC Click, 5 27 2014: https://www.bbc.co.uk/programmes/p01zkqq0

(295). Ariel Schwartz A Portable Metabolism Tracker To Tell You Why You’re Fat, Scientific American, Feb. 2013: http://www.scientificamerican.com/article.cfm?id=a-portable-metabolism-tracker-to-te-2013-02

(296). Nosta John, Don’t Only Count Calories and Steps, Your Metabolism is Key!, Forbes, Feb. 8, 2013: https://www.forbes.com/sites/johnnosta/2013/02/08/dont-only-count-calories-and-steps-your-metabolism-is-key/#4af686c55517

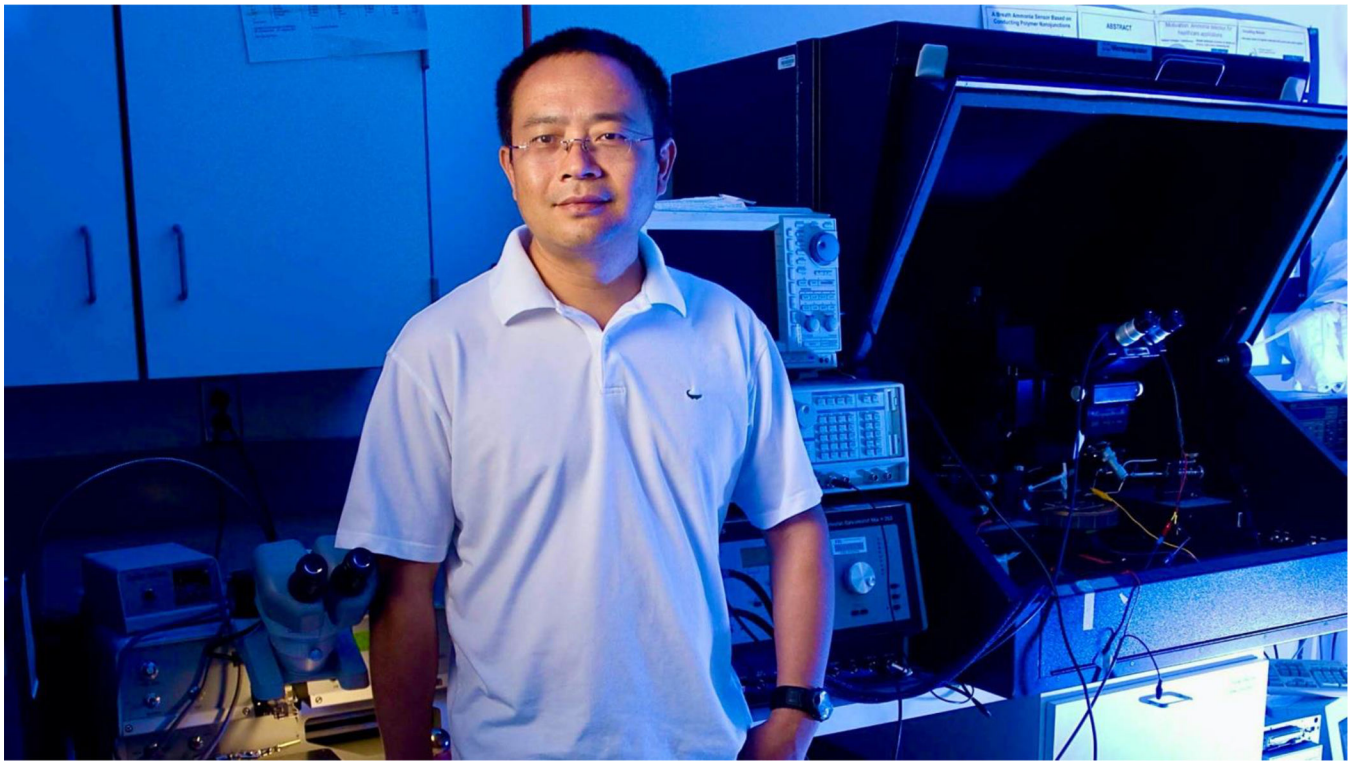

Figure 1.
Professor Nongjian Tao in his laboratory in 2008. Image credit: The Biodesign Institute at Arizona State University.

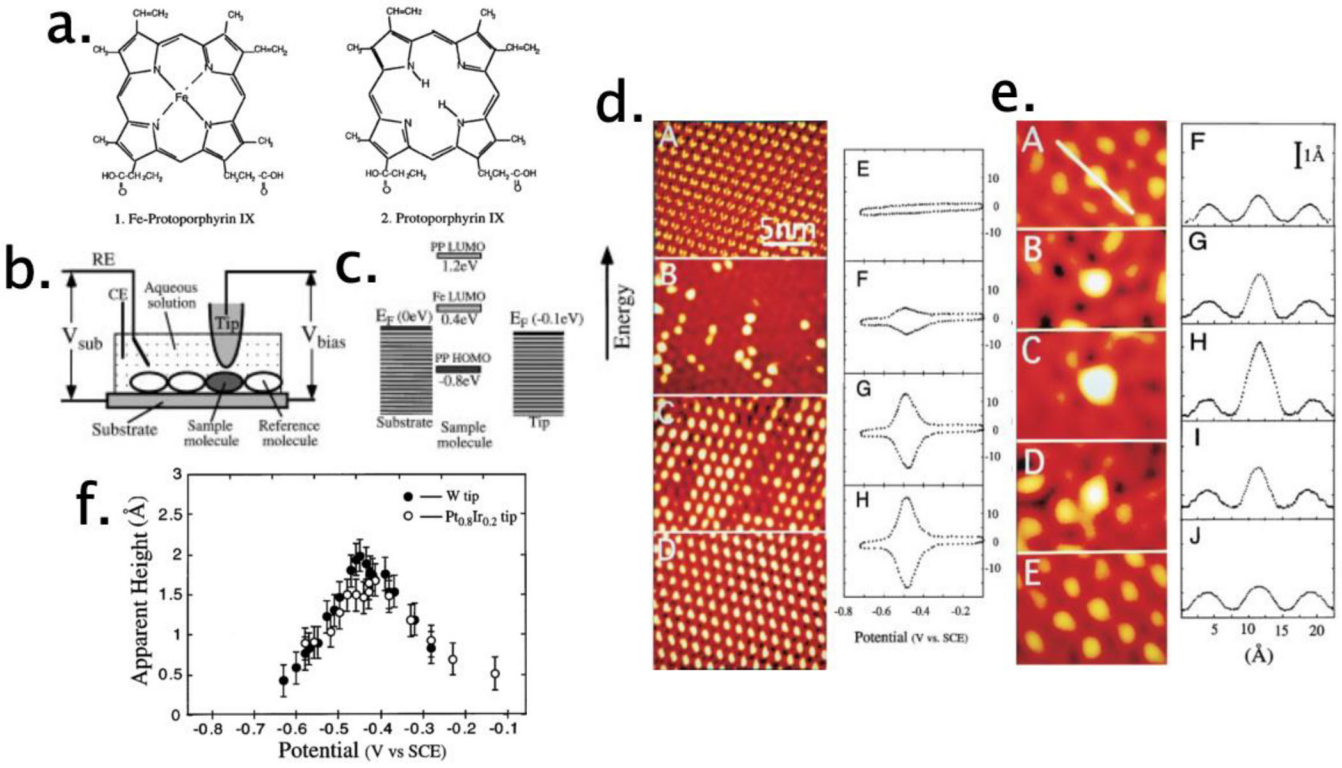

Figure 2.

a) Iron protoporphyrin (FePP, left) and protoporphyrin (PP, right) molecules. b) Schematic diagram of a scanning tunneling microscope (STM) with control of the electrochemical potential of the tip and surface for investigations of single-molecular electron transfer. c) Energy level diagrams of Fe(III)-protoporphyrin IX and protoporphyrin IX and their relation to the Fermi levels of the substrate and tip. d) STM images of FePP/PP mixed monolayers on graphite containing FePP and PP at the ratio of 0:1 (A), 1:4 (B), 4:1 (C), and 1:0 (D). (E)–(H) are the corresponding cyclic voltammograms, e) STM image of FePP molecule embedded in an ordered matrix of PP molecules when the substrate was held at −0.15 (A), −0.30 (B), −0.42 (C), −0.55 (D), and −0.65 V (E), *versus* SCE ref. electrode. (f) Apparent height of FePP relative to PP as a function of the substrate potential *via* Pt-Ir tip and W tip. Figures a–d reprinted with permission from ref[87]. Copyright 1996 American Physical Society.

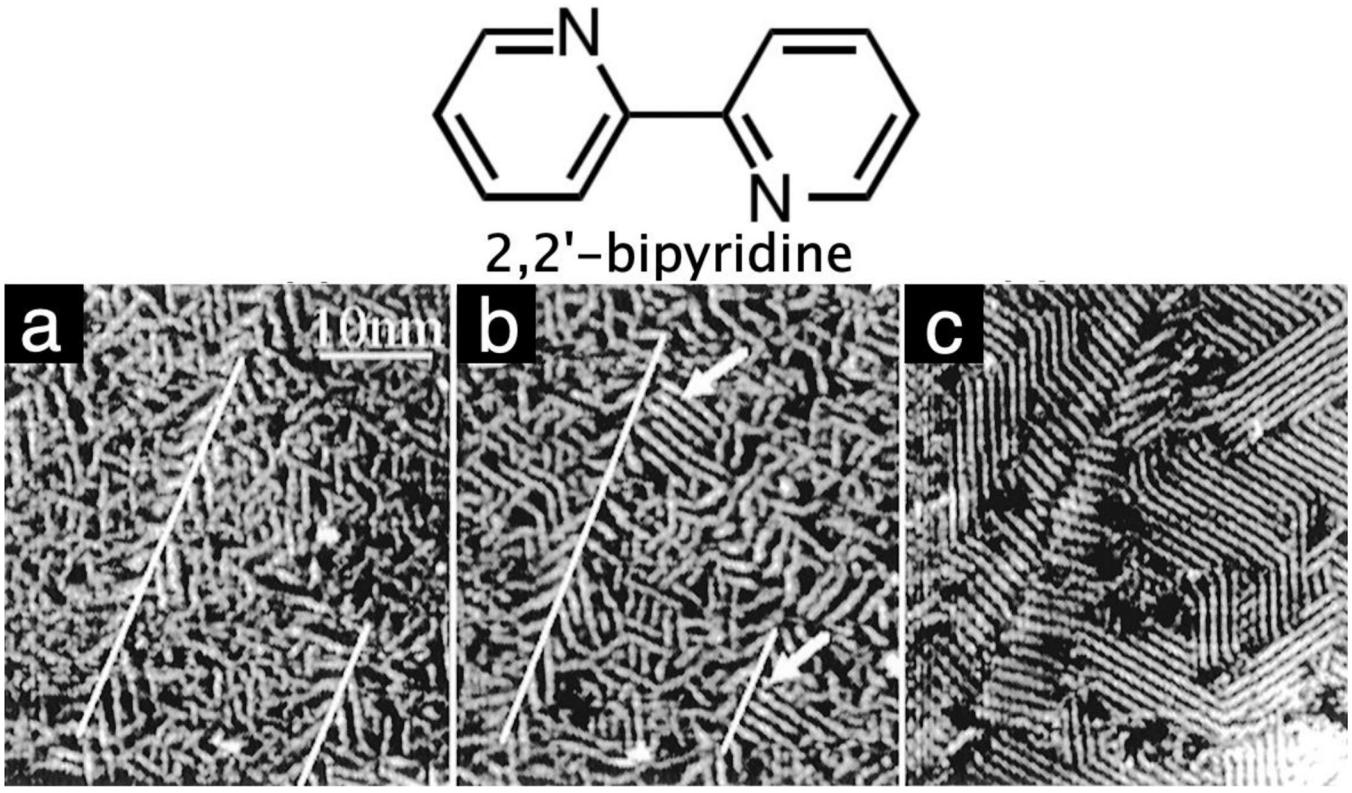

Figure 3.

Potential-induced disorder–order transition in a 2,2’-bipyridine monolayer on reconstructed Au(111). Images a, b, and c were obtained at sample potentials of 0.11 V, 0.24 V, and 0.38 V *versus* SCE, respectively, in aqueous 0.10 M $NaClO_4$. Lines in a and b indicate the direction of the reconstruction strips. Arrows in b point to the formation of the ordered phase as the potential is raised to 0.24 V. Reprinted from ref[94]. Copyright 1996 American Chemical Society.

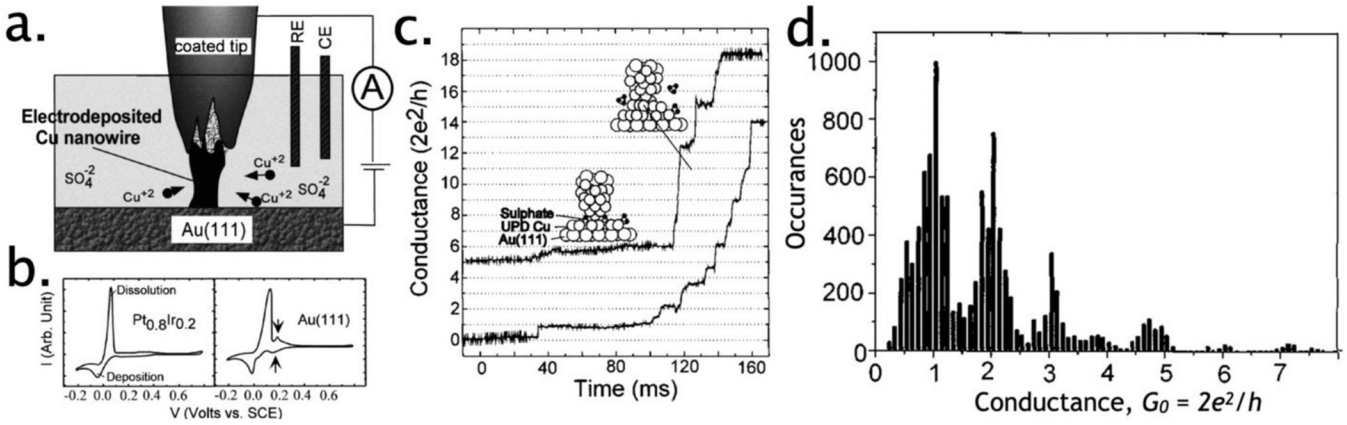

Figure 4.

Quantum transport in metallic nanowires. a). Schematic drawing of the experimental setup. b,c) Plots of deposition/dissolution current *versus* the potential for an Au(111) substrate (b, left) and a segment of $Pt_{0.8}Ir_{0.2}$ wire (the tip material, b, right) are obtained by sweeping the potential linearly at a rate of 50 mV/s. Note that the actual deposition/dissolution current for the coated tip used in the experiment is too small to be measured, c) As Cu is deposited onto the tip, the growing front touches the substrate electrode, resulting in a stepwise increase in the conductance. The top curve is shifted upward by 5 G_0 for clarity. The tip and the substrate potentials were held at 30 and 25 mV, respectively. d) Conductance histogram for Cu nanowires fabricated by electrochemical deposition and dissolution at room temperature. Reprinted with permission from ref[115]. Copyright 1998 American Institute of Physics.

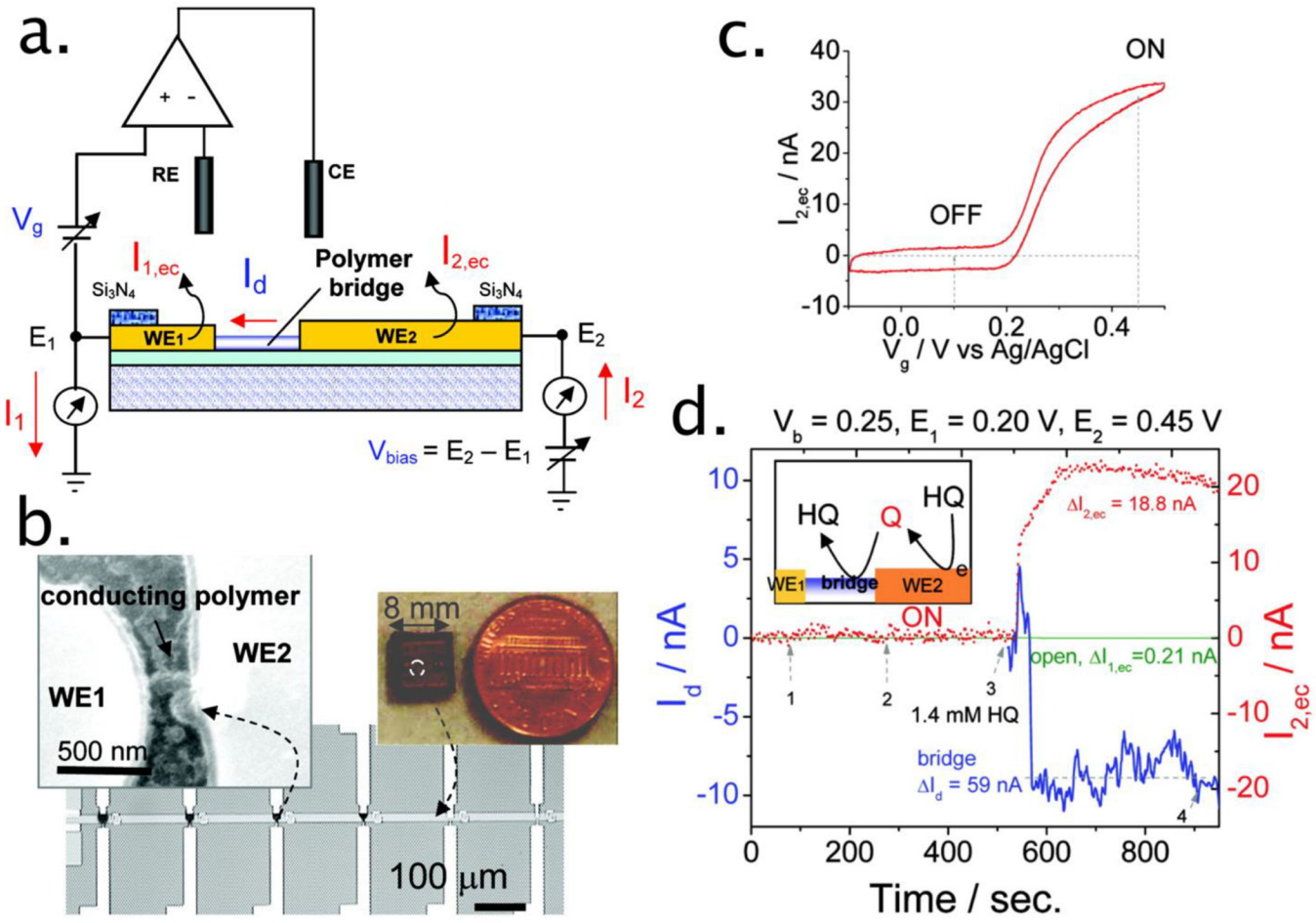

Figure 5.

(a) Schematic illustration of a hybrid amperometric and conductometric sensor. WE1 and WE2 represent two working electrodes (source and drain electrodes) connected with a conducting polymer bridge. RE and CE are reference and counter electrodes, respectively. The electrochemical gate potential (V_g) E_1 is applied between the drain electrode (WE_1) and RE, and a bias voltage (V_{bias}) is applied between WE_1 and WE_2. (b) Optical and scanning electron microscope images of the device made of an array of polymer bridges on a silicon chip. (c) Cyclic voltammogram of 3.9 mM hydroquinone (HQ) on polyaniline-modified microelectrode at 60 mV/s. (d) ΔI_d and $\Delta I_{2,ec}$ simultaneously recorded during the injections of supporting electrolyte (1–2) and 1.4 mM HQ (3) to a close (bridge) and open polymer bridge (open) amperometric and conductometric device. V_{bias}) 0.25 V and E_2) 0.45 V. Inset of (d) illustrates the reaction mechanism in a close polymer bridge device. Reprinted from ref[34]. Copyright 2007 American Chemical Society.

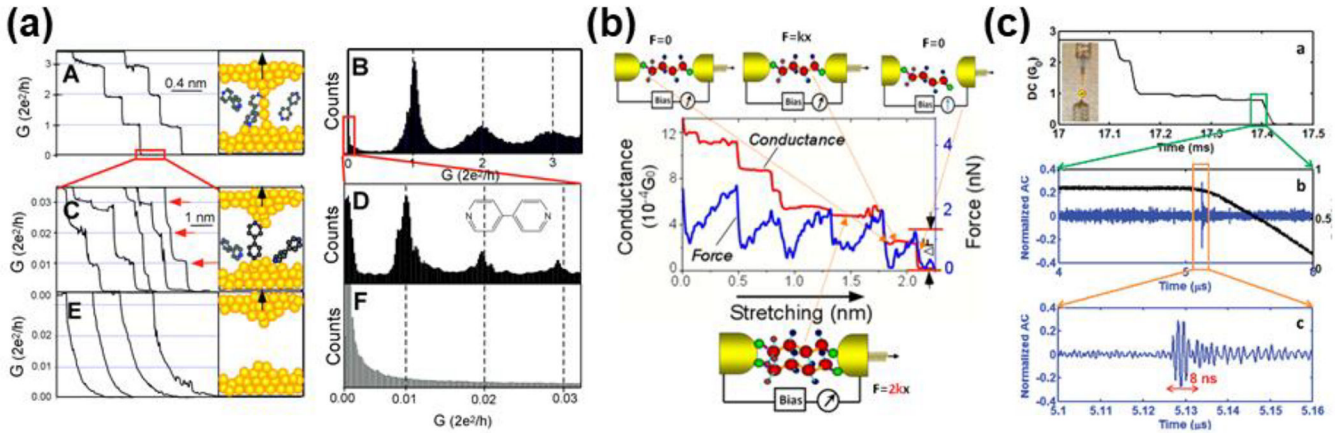

Figure 6.

The scanning tunneling microscopy-break junction (STM-BJ) method. (a) STM-BJ using 4’4’-bipyridine molecules. Reprinted with permission from ref 293. Copyright 2003 American Association for the Advancement of Science. (b) Conductive atomic force microscopy measurement of Au-thiol binding in Au–octanedithiol–Au molecule junction. Reprinted from ref 38. Copyright 2003 American Chemical Society. (c) AC-modulation of molecular junctions. Reprinted from ref 12. Copyright 2011 American Chemical Society.

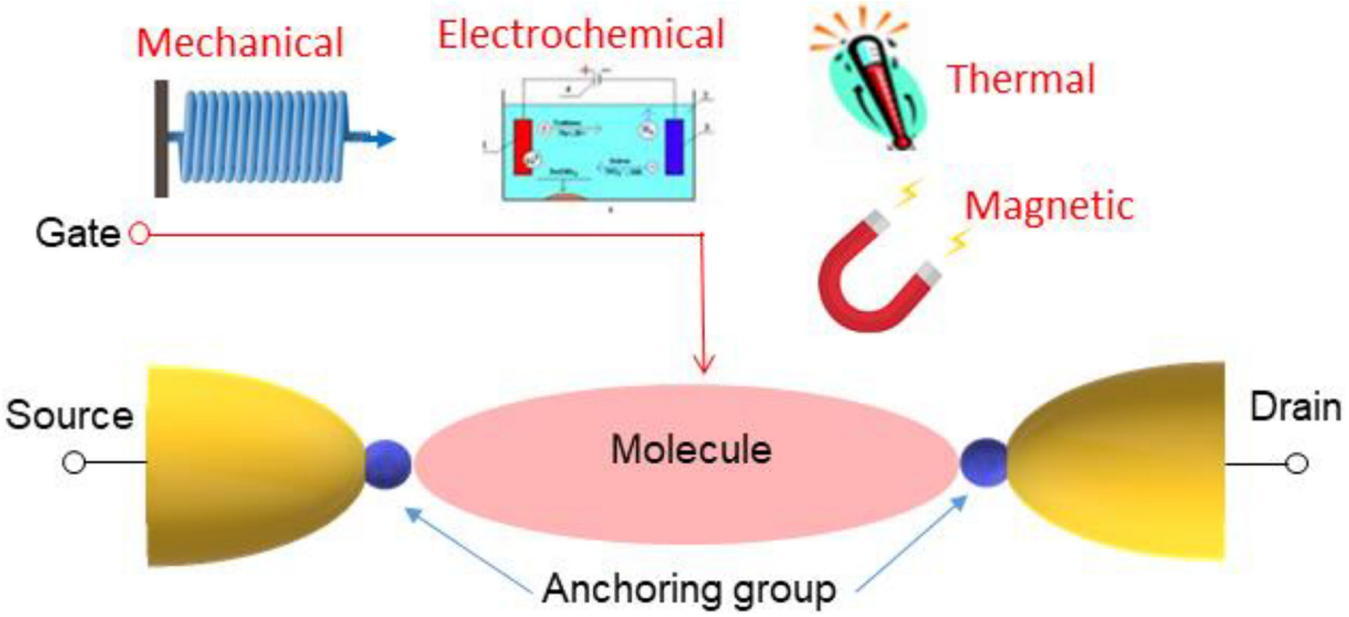

Figure 7.
Schematic illustration of controlling electron transfer in molecular junctions by mechanical, electrochemical, thermal, and magnetic gating.

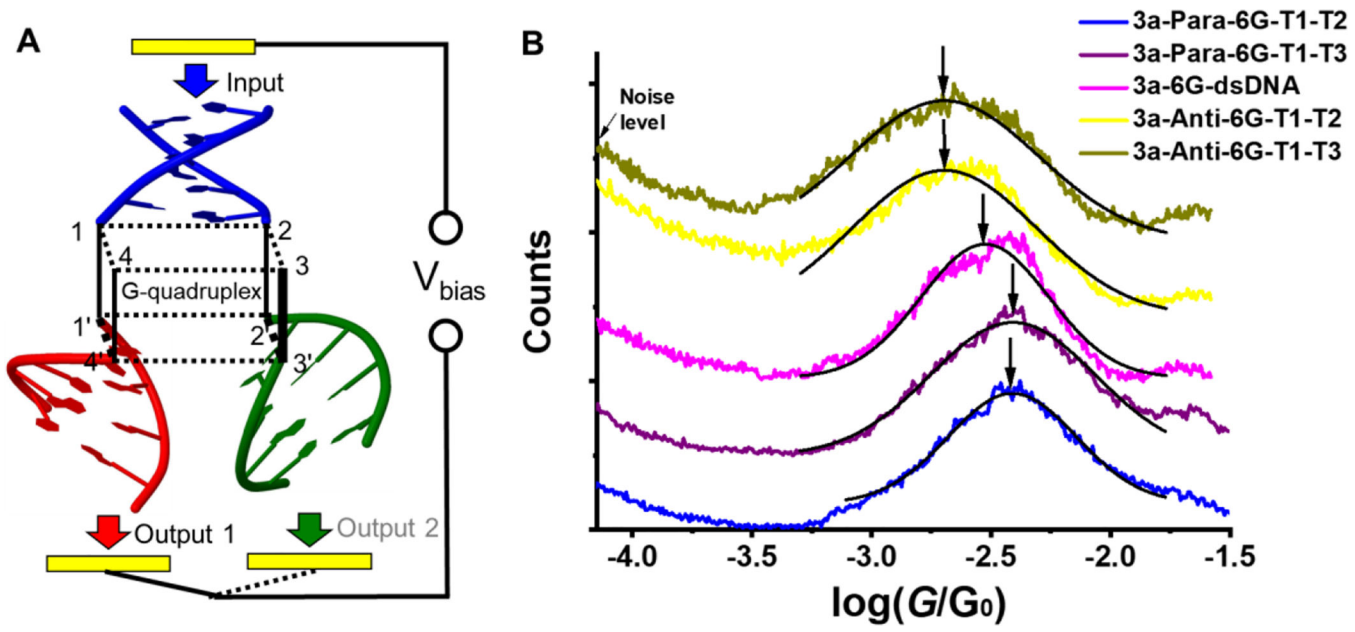

Figure 8.

Design and testing of a G-quadraplex-based current splitter. (A) Schematic of the current-splitting element placed between two electrodes. The G4 element (black) plus 3 DNA duplexes are held between an Au tip and an Au substrate in a break-junction configuration. (B) Conductance histograms of the quadruplex 3 with six layers of guanines. The different conductance histograms represent whether the strands are arranged in an antiparallel or parallel configuration and which of the three duplex terminals (T1, T2, T3) have thiols to bind to the electrodes. The conductance values (*x*-axis) are similar for all the DNA structures. For clarity, each histogram was shifted vertically to avoid overlap. Reprinted with permission from ref[232]. Copyright 2018 Springer Nature.

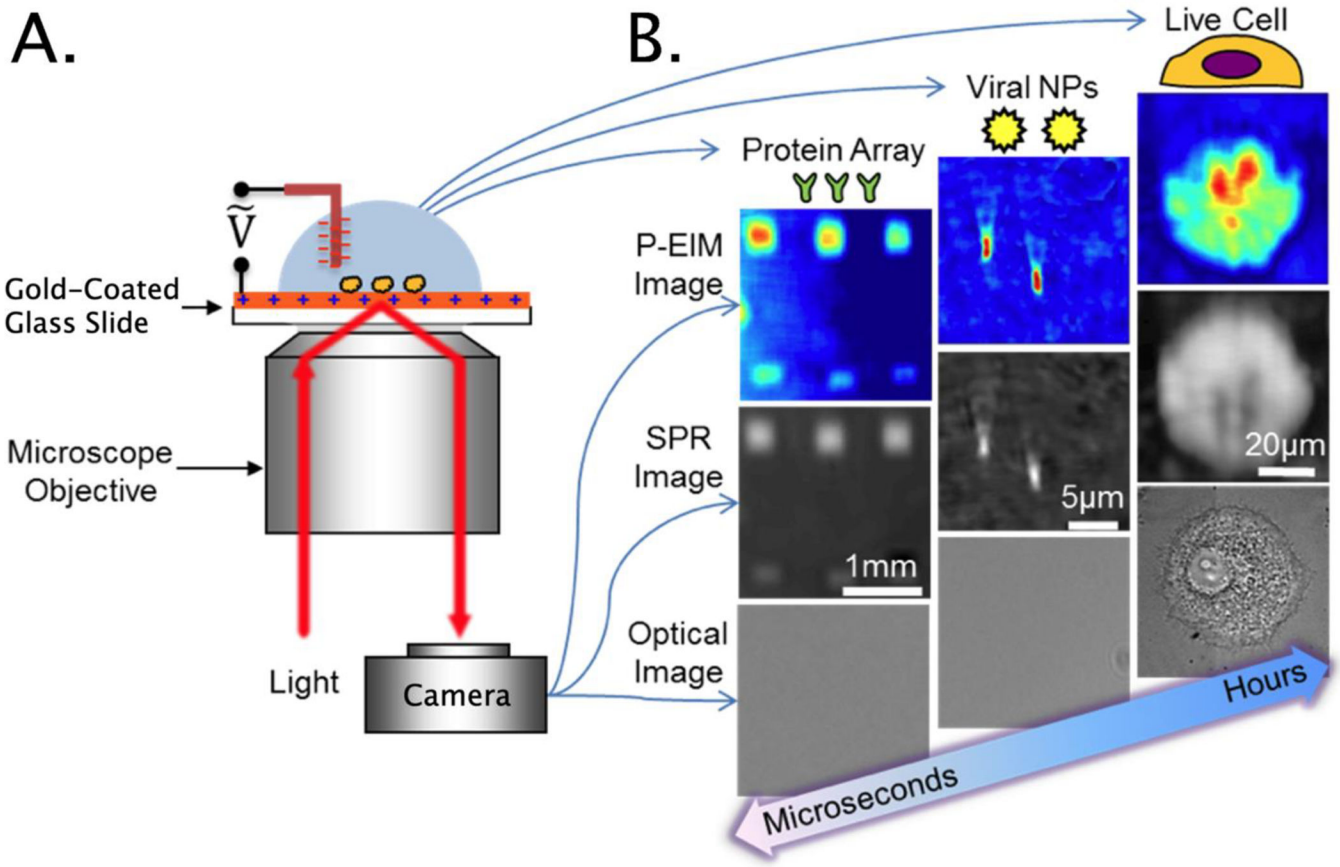

Figure 9.

Principles and applications of plasmonic-based electrochemical impedance microscopy (P-EIM) microscopy. (A) Schematic of P-EIM imaging principle: Surface plasmon waves are created optically with a laser or light-emitting diode beam incident on the metal film *via* a prism or high-numerical-aperture objective at a resonant angle, and the reflected beam creates a surface plasmon resonance microscopy (SPRM) image. The resonant angle is sensitive to changes in refractive index near the metal surface, which is widely used to study molecular binding processes. In addition, the resonance angle is also sensitive to surface charge density, which produce the electrochemical impedance image when an AC voltage is applied to the surface. (B) optical, SPRM and P-EIM images of a protein microarray, viral nanoparticles (NPs), and a mammalian cell.

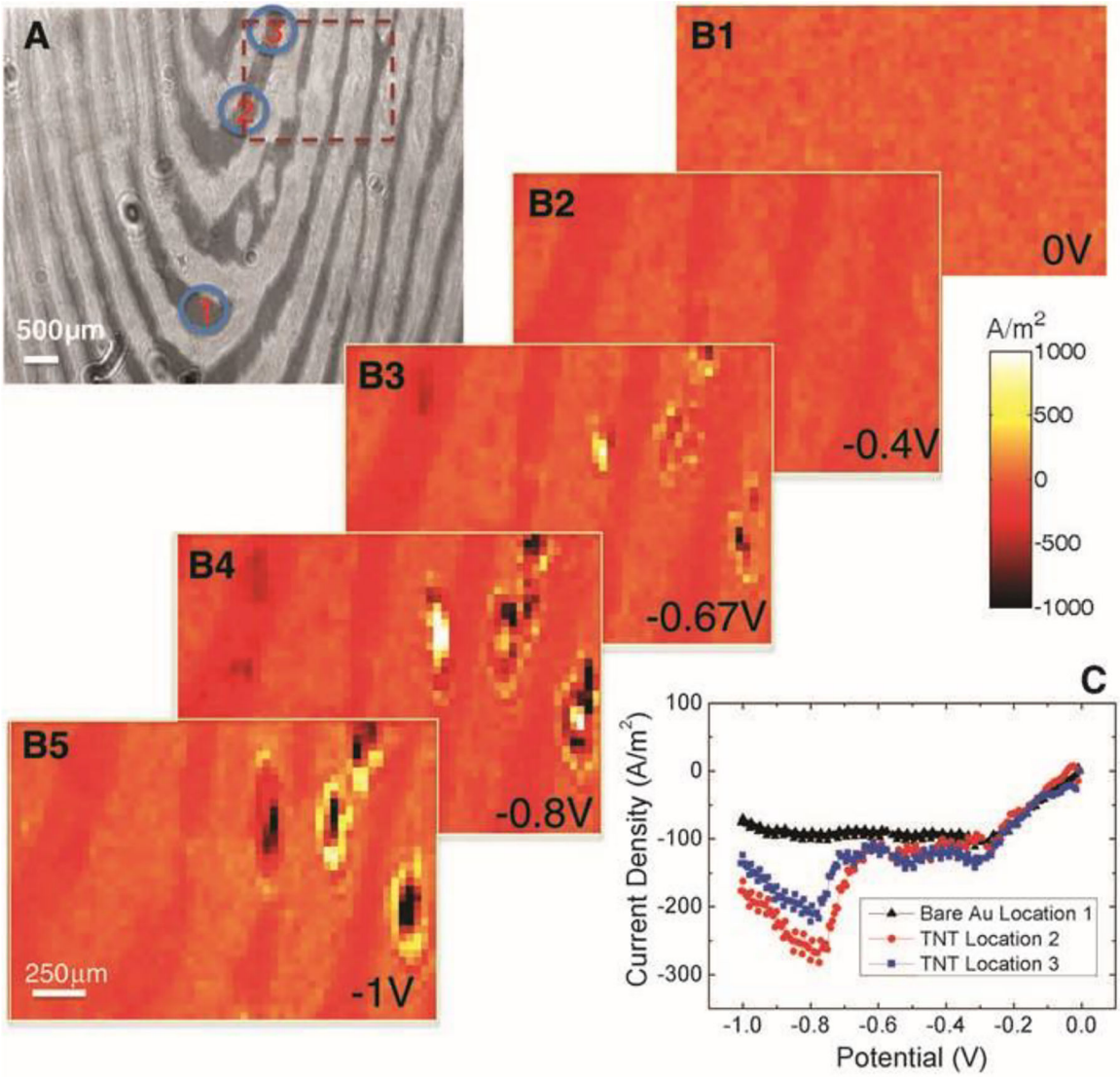

Figure 10.

Detection of TNT traces on a fingerprint using the electrochemical current imaging technique. (A) Surface plasmon resonance image of a fingerprint. (B1–B5) Five snapshots recorded while sweeping the potential negatively from 0 to −1.0 V at a rate of 0.05 V/s. The appearance of the “spots” is due to the reduction of TNT particulates. (C) Local voltammograms of the regions with (blue and red dots) and without (black dots) TNT particulates. The electrolyte is 0.5 M KCl. Reprinted with permission from ref[23]. Copyright 2010 American Association for the Advancement of Science.

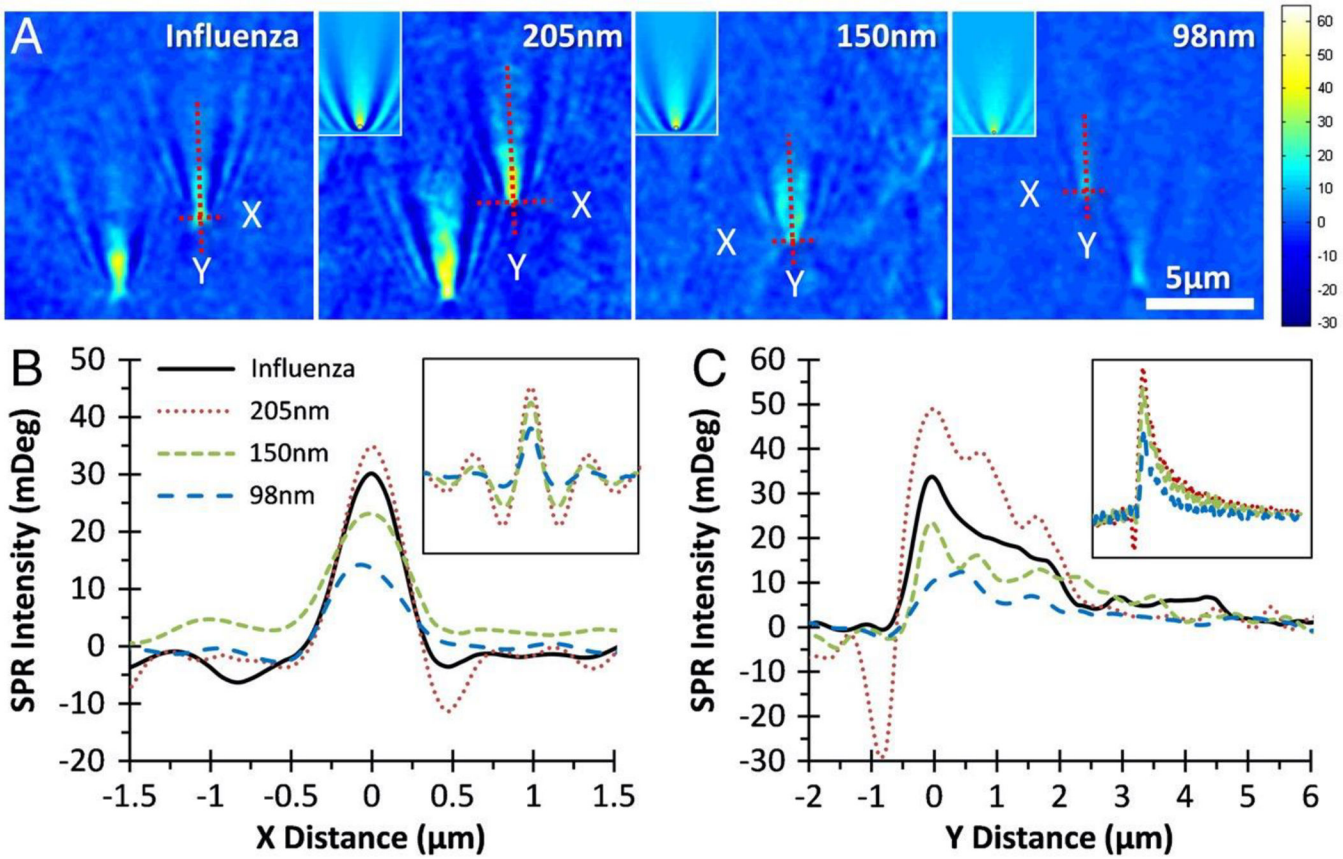

Figure 11.

(A) Surface plasmon resonance microscopy (SPRM) images of H1N1 influenza A virus and three different sized silica nanoparticles in phosphate-buffered saline (PBS) buffer. (Insets) Nanoparticle images generated by numerical simulation. (B and C) The SPR intensity profiles of selected particles along X and Y directions (indicated by dashed lines in A, respectively. (Insets) Corresponding profiles from simulated images. Reprinted with permission from ref[28]. Copyright 2010 Wang *et al.*

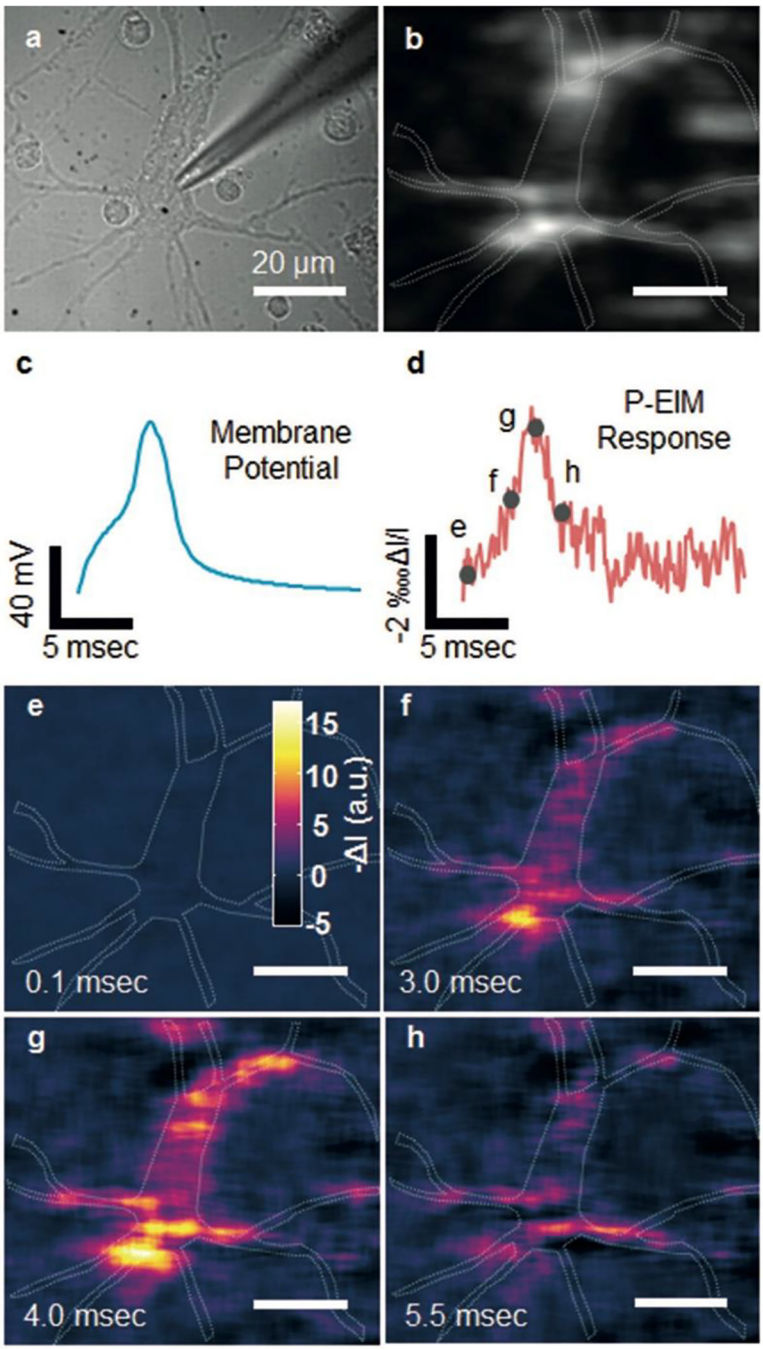

Figure 12.

Plasmonic imaging of action potential in single neurons. a) Bright-field and b) plasmonic images of a hippocampal neuron, where the dashed lines mark the edge of a neuron. c) Patch clamp recording of action potential and d) simultaneous plasmonic-based electrochemical impedance microscopy (P-EIM) recording of action potential of the whole cell (frame rate of 10000 fps). To clearly illustrate the data, we normalized the intensity change DI with mean intensity I, and plotted the plasmonic intensity in negative intensity change for fair comparison. e–h) Snapshot P-EIM images of action potential at the moments marked by the

gray spots in (d). The P-EIM images were averaged over 90 cycles of repeated action potential firing at 23 Hz repeat rate to reduce random noise. Reprinted with permission from ref[285].

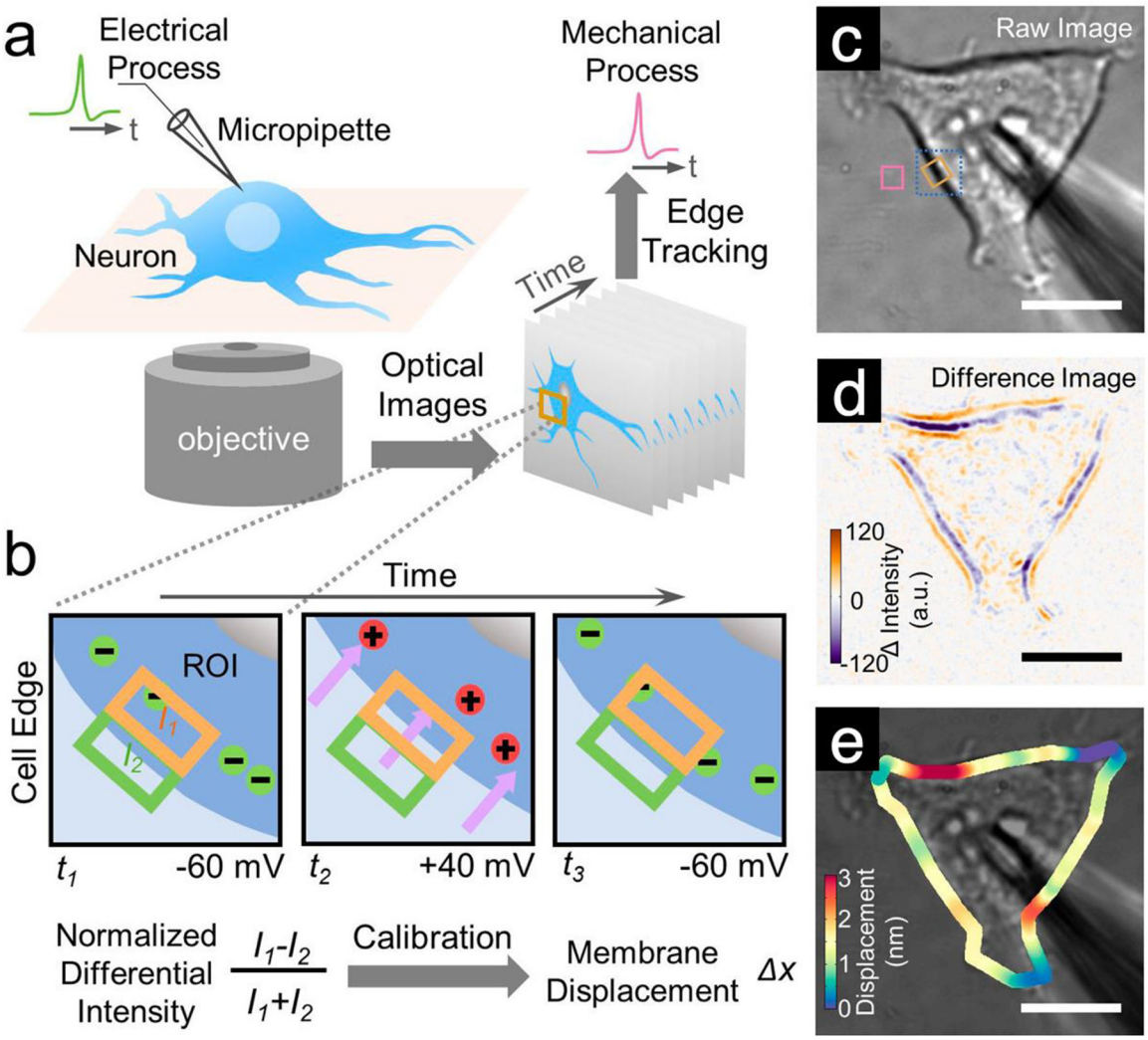

Figure 13:

Tracking sub-nm membrane displacement accompanying action potential in single mammalian neurons. a) Experimental setup showing a hippocampal neuron cultured on a glass slide mounted on an inverted optical microscope, which is studied simultaneously with the patch clamp configuration for electrical recording of the action potential, and optical imaging of membrane displacement associated with the action potential. b) Imaging and quantification of membrane displacement with a differential detection algorithm that tracks the edge movement of a neuron. c) Bright-field image of a HEK293T cell and a micropipette used to change the membrane potential. d) Difference image of the entire cell showing cell edge displacement and local variability (intensities for the orange and purple bands) of the displacement. e) Membrane displacement map obtained from the differential detection algorithm. Scale bar in (c, d, e): 10 μm. Reprinted from ref[293]. Copyright 2018 American Chemical Society.

Figure 14.

Wireless wearable chemical sensor based on tuning fork sensors for selective and real-time detection of hydrocarbons (traffic pollutants) and acid vapors with sensitivity of ppb – ppm range, spatial resolution, and signal processing based on a cell phone app. The device was used to monitor the exposure of individuals to traffic pollutants.

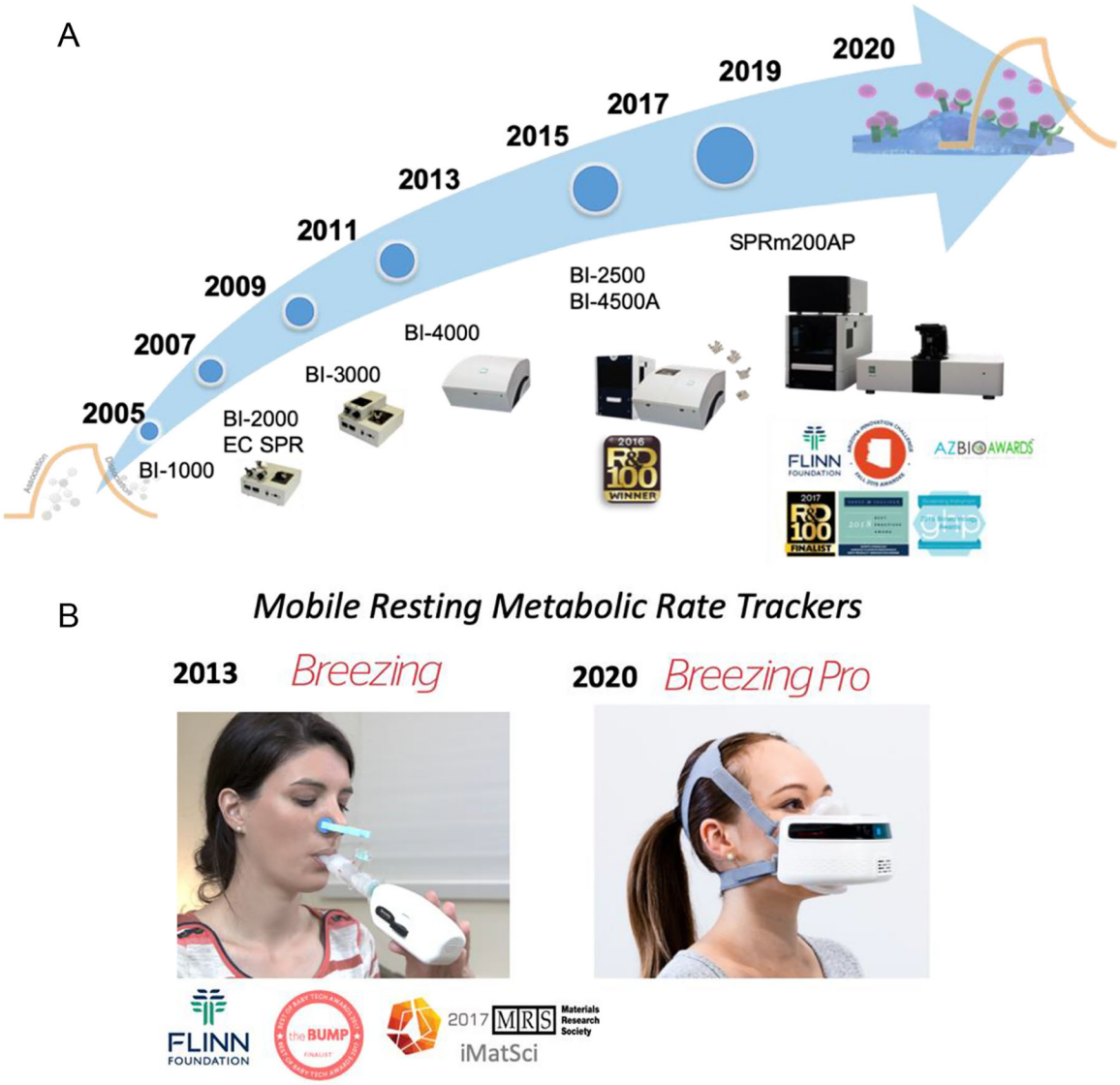

Figure 15.

Evolution of products manufactured by: (A) Biosensing Instrument Inc. (https://biosensingusa.com/), (B) TF Health Co., dba Breezing (https://breezing.com/).